Probiotics and Antimicrobial Proteins
https://doi.org/10.1007/s12602-025-10624-0

RESEARCH

Characteristics of Two *Saccharomyces cerevisiae* Strains and Their Extracellular Vesicles as New Candidates for Probiotics

Aleksander Gryciuk[1] · Małgorzata Milner-Krawczyk[1] · Marta Rogalska[1] · Artur Krzysztof Banach[2] · Ewa Sitkiewicz[3] · Magdalena Bakun[3] · Magdalena Edyta Świadek[4] · Jolanta Mierzejewska[1]

Accepted: 29 May 2025

Abstract

There is a huge disparity between the number of bacterial and yeast probiotics in favor of the former. The latest reports indicate that extracellular vehicles (EVs) play a significant role in probiotic mechanisms. In the present work, we compared the probiotic properties of *Saccharomyces cerevisiae* strains (WUT3 and WUT151), which have never been previously characterized in this context, with commercial probiotic yeast—*Saccharomyces cerevisiae var. boulardii* CNCM-745. Notably, WUT3 and WUT151 reacted more mildly to the unfavorable simulated environment of saliva, stomach, small, and large intestines. As a result, we confirmed that WUT3 and WUT151 were superior to *S. boulardii* in terms of probiotic properties. Then, we performed a complex analysis of their EVs, isolated by a multistep filtration process. The nanoparticle tracing analysis showed no significant difference in the diameter of the vesicles between the strains. MTT studies confirmed that EVs are not toxic against normal human colorectal cell lines CCD-18 Co and CCD 841 CoN. However, toxicity was observed against the HT-29 cancer line. By staining EVs with Nile Red, we successfully visualized EVs–cell interactions. Finally, we explored the profile of proteins transported with the EVs, identifying a significant overrepresentation of extracellular proteins. Based on comparison with other proteomic data, we selected marker proteins for *S. cerevisiae* EVs. This knowledge will be helpful for further studies on tracking the transfer of the protein cargo of yeast EVs to human cells using, for instance, specific antibodies to these marker proteins.

Keywords EVs · *Saccharomyces cerevisiae* · *Saccharomyces boulardii* · Gene ontology · Biomarker

Introduction

The definition of probiotics has evolved over the years. In 1960, this term was used as the opposite of antibiotics, meaning this substance can assist other microorganisms' growth. Only 20 years later, the definition was improved, indicating that bacteria are probiotic agents. In 2012, the WHO approved the following definition of a probiotic, which is still used today: live microorganisms that, when administered in adequate amounts, confer a health benefit on the host [1]. Those benefits relate to the impact on the host microbiota and positive immune system stimulation [2, 3]. Even though the positive effects of probiotics on human health have been known for a long time, they are still not considered medicines [4].

Probiotic strains should fulfill several requirements. First, they must be adapted to the harsh conditions in the gastrointestinal tract, exhibiting resistance to low pH, bile salts, and pancreatic fluids [4, 5]. Growth at 37 °C is also

✉ Aleksander Gryciuk
aleksander.gryciuk.dokt@pw.edu.pl

✉ Jolanta Mierzejewska
jolanta.mierzejewska@pw.edu.pl

[1] Microbiology and Bioengineering Laboratory, Faculty of Chemistry, Warsaw University of Technology, Warsaw, Poland

[2] MicroBioRobotic Systems Laboratory, Institute of Mechanical Engineering, École Polytechnique Fédérale de Lausanne, Lausanne, Switzerland

[3] Mass Spectrometry Laboratory, Institute of Biochemistry and Biophysics, Polish Academy of Sciences, Warsaw, Poland

[4] Laboratory of Electron Microscopy, Nencki Institute of Experimental Biology, Polish Academy of Sciences, Warsaw, Poland

Published online: 13 June 2025

recommended, as this is the inside temperature of the human body [6]. Probiotics should also adhere to the mucosa and intestinal epithelial cells to effectively colonize the intestines. Probiotics cannot display any pathogenic properties, e.g., hemolytic activity. Therefore, potential new strains should be part of the Generally Recognized As Safe family (GRAS) [4].

Bacteria dominate probiotics in both industry and research [7]. More than 40,000 articles related to probiotics were published in Science Direct between 2019 and 2024. Approximately 57% of these publications focused exclusively on bacteria, while only 1.8% mentioned yeast without reference to bacteria. This illustrates a significant research gap in the study of yeast as standalone probiotic organisms. The online "probiotics database" contains names of the most important probiotic strains examined in clinical trials. There are 21 strains of 10 bacterial species and only one yeast species—*Saccharomyces boulardii* (SB) [8]. Such a small amount of yeast probiotics is astounding because yeast has always accompanied humans in fermented foods. Moreover, many yeast strains meet entirely the requirements for probiotics. Nevertheless, more advanced studies on probiotic yeast are rarely reported.

The taxonomy classification of *S. boulardii* (SB) has been the subject of intense discussion. Historically, isolated in 1923 by Henri Boulard from lychee, it was classified as an individual yeast species [5]. One of the reasons for this separation was the inability of *S. boulardii* to metabolize galactose and produce ascospores, which is typical for *Saccharomyces cerevisiae* (SC). In the late'90 s, SDS-page electrophoresis of restriction fragments was the standard taxonomy technique. This analysis showed differences in SB and SC's model class boundaries [9]. From a physiological point of view, generally SB is more resistant to high temperatures and grows faster than SC [5, 10]. Nevertheless, due to the high genomic and structural similarity, *boulardii* was finally included in the *cerevisiae* species, and its present full taxonomy name is *Saccharomyces cerevisiae var. boulardii* [6, 11].

S. boulardii probiotic properties were proved in double-blind clinical trials [5]. It is the only yeast approved for use in pharmaceutical products. SB commonly treats retroviral and bacterial diarrhea and inflammatory bowel disease [6, 12]. There are 42 completed and 7 starting (2 not yet recruiting) clinical trials on some SB strains. Almost 24% of completed trials were in phase IV [13].

Every type of live cell produces extracellular vehicles (EVs). Those lipid bilayer particles have sizes ranging from 20 to 500 nm and are unable to self-replicate [14, 15]. Cells use them to communicate or respond to changes in the environment. To date, the protein and genetic profiles of the yeast EVs have been mainly studied for pathogenic species, first in 2007 for *Cryptococcus neoformans*. As a result of those studies, it was found that yeast EVs can interact with human cells [16]. It is intuitive to state that EVs must play an important part in yeast probiotic mechanisms. Examining and characterizing yeast EVs is essential in developing new generation probiotics. The knowledge of EVs biomarkers, their size, and other physical and chemical properties may help in further research to develop smart probiotics, transporting bioactive compounds directly to the host cells. This could revolutionize modern drug delivery systems.

This work examines the in vitro probiotic properties of two *S. cerevisiae* strains and their EVs. Based on a complex comparison of new strains with commercial *S. cerevisiae var. boulardii* CNCM I-745, we report some important advantages in the probiotic properties of these yeasts.

Materials and Methods

Yeast Strains and Culture Conditions

Saccharomyces cerevisiae WUT3 and WUT151 strains were isolated from fermented milk drinks of Turkish and Kyrgyzstan origin, respectively, and deposited in the Warsaw University of Technology (WUT) Yeast Collection (wut-yeastcollection.pw.edu.pl). The WUT3 strain has previously been reported to be an attractive producer of 2-phenylethanol [17]. *Saccharomyces cerevisiae var. boulardii* CNCM I-745 (SB, *S. boulardii*) from commercially available probiotic Enterol® (Biocodex, Poland) was used as a reference. Yeasts were seeded on the SAB agar (Sabouraud Dextrose, BioMaxima, Poland) via spreading a sample taken directly from frozen glycerol stock (− 80 °C, WUT3 and WUT151) or a small amount of Enterol® (SB). Plates were incubated at 37 °C for 48 h, and then single colonies were used for studies.

Assimilation ability was tested on yeast nitrogen base (YNB with ammonium sulfate and without amino acids, Conda, Spain) supplemented with a single carbon source—glucose (Chempur, Poland), sucrose (AppliChem, Germany), galactose (Carl Roth, Germany), maltose (BioShop, Canada), glycerol (BioShop, Canada), or ethanol (POCH, Poland) at a final concentration of 2% (w/v). Hemolytic and proteolytic activities were established by spreading single yeast colonies on the BD Columbia Agar with 5% sheep blood plates (Becton Dickinson, USA) and nutrient agar (BioMaxima, Poland) supplemented with 10% (v/v) skimmed milk (Piątnica, Poland), respectively. *Streptococcus aureus* ATCC6538 was used as a positive control. The seeded plates were incubated at 37 °C for 2 days.

To estimate yeast growth rates, the overnight cultures of WUT3, WUT151, and SB were prepared by inoculation of 5 ml of liquid SAB or YPD ($1\%_{w/v}$ yeast extract (BioMaxima, Poland), $2\%_{w/v}$ bacteriological peptone (BioMaxima, Poland), and $2\%_{w/v}$ glucose (Chempur, Poland))

and incubation at 37 °C for 18–20 h with shaking at 240 rpm (Benchtop shaker SI-600R LabCompanion, USA). Then, they were diluted to an initial optical density of 0.1 ± 0.05 at a wavelength of 600 nm (OD600; spectrophotometer UV-1800 PC, AOE Instruments, China) in 150 ml of SAB medium, in two independent biological repeats. Then, cultures were conducted for 48 h at 37 °C and 220 rpm. Yeast growth was monitored by measuring OD600, spreading ten-fold serial dilutions on the SAB agar plates, and calculating CFU (colony forming units). At the end of 48 h incubation, 40 ml of yeast culture was centrifuged (5000 × *g*, 5 min, Eppendorf Centrifuge 5804 R). After removing the liquid, the biomass was dried at 50 °C for 72 h and weighed. The maximum specific growth rate (μ_{max}) of yeast was calculated using linear regression (Origin Pro 2021) for the logarithmic growth phase, for data points in the range of 2–8 h, using the formula:

$$\ln\left(\frac{OD_{600_t}}{OD_{600_{t_0}}}\right) = \mu_{max}t - \mu_{max}t_0$$

where OD_{600} is the optical density of yeast sample in a given time or at the beginning of the logarithmic phase, t is time [h], t_0 is the time when logarithmic phase started (2 h).

Biomass/substrate coefficient (Y_{XS}) was calculated assuming that dextrose from SAB medium was the only source of carbon and it was entirely and only used for biomass production, using the formula:

$$Y_{XS} = \frac{X}{S}$$

where X is the dry mass of yeast, and S is the initial dextrose mass in the 40 ml of media.

The generation time (t_G) was derived directly from the definition of the specific growth rate:

$$\ln\left(\frac{2 \bullet X}{X}\right) = \mu_{max}\left(t_{2X} - t_X\right) \overset{t_{2X}-t_X=t_G}{\rightarrow} t_G = \frac{\ln(2)}{\mu_{max}}$$

To determine yeasts' diameter distribution, 10 µl of WUT3, WUT151, or SB overnight cultures were spotted on the glass slide. Microscopic observations were carried out with 600 × magnification using a Nikon Eclipse Ni fluorescence microscope, with Plan Fluor 60 ×/0.85 lens, CFI 10 ×/22 ocular, and Nikon DS-Fi3 camera. Images were captured with NIS Elements DR ver. 5.30.04 software. A total of 26 images in random positions were taken for each strain. Then, the diameter of at least 500 non-budding cells was counted using ImageJ ver. 1.54j software. Statistics and error propagation were calculated as described in Supp. Data 1.

Yeast Survival in the Gastrointestinal Environment

To simulate the path the yeast must take in the gastrointestinal tract, the yeast suspension was transferred from one simulation fluid to another in the order and incubation time occurring in the human gastrointestinal tract. Thus, 8 ml of overnight WUT3, WUT151, and SB cultures in SAB were washed with 8 ml of sterile tap water (4000 × *g*, 10 min) and then suspended in the same amount of sterile water, giving an initial cell suspension. A total of 5 ml of 2 × concentrated simulated gastrointestinal fluids (see final concentrations in Table 1) were placed in individual sterile glass tubes: simulated saliva fluid (SSF), simulated gastric fluid (SGF), simulated intestines fluid (SIF), and simulated colon fluid (SCF).

The schematic workflow of the experiment is shown in Fig. 1. Briefly, 5 ml of initial cell suspension (1) was added to fresh SSF fluid (2) and incubated at 37 °C for 2 min with shaking at 240 rpm. Then, 5 ml of SSF suspension was transferred to the fresh SGF (3) and incubated at 37 °C for 1 h, 240 rpm. After incubation, 5 ml of SGF suspension was transferred to the fresh SIF (4) for the next incubation at 37 °C for 2 h, 240 rpm. Finally, 5 ml of SIF suspension was transferred to the fresh SCF (5) and incubated at 37 °C

Table 1 Gastrointestinal simulated fluids composition based on [18, 19] with modifications. The table shows the final concentrations in the experiment after dilution 1:1 with the yeast suspension from the preceding intestinal segment

Ingredient	SSF	SGF	SIF	SCF
KCl (Chempur, PL)	1.1 mg/ml	0.5 mg/ml	0.5 mg/ml	0.2 mg/ml
KH_2PO_4 (Polaura, PL)	0.5 mg/ml	0.1 mg/ml	0.1 mg/ml	0.24 mg/ml
$NaHCO_3$ (Chempur, PL)	1.1 mg/ml	2.1 mg/ml	7.1 mg/ml	1.44 mg/ml
NaCl (Chempur, PL)	-	2.5 mg/ml	2.2 mg/ml	8 mg/ml
$MgCl_2$ (Chempur, PL)	0.03 mg/ml	0.02 mg/ml	0.07 mg/ml	-
$(NH_4)HCO_3$ (Merck, DE)	0.006 mg/ml	0.04 mg/ml	-	-
$CaCl_2 \bullet 2\ H_2O$ (Chempur, PL)	0.2 mg/ml	0.02 mg/ml	3 mg/ml	-
Pepsin (Merk, DE)	-	4000 U/ml	-	-
Pancreatin (Merk, DE)	-	-	2 mg/ml	-
Bile salts (Merk, DE)	-	-	5 mg/ml	-
SAB (BioMaxima, PL)	-	-	-	30 mg/ml
pH	7	3	7	7

PL, Poland; DE, Germany

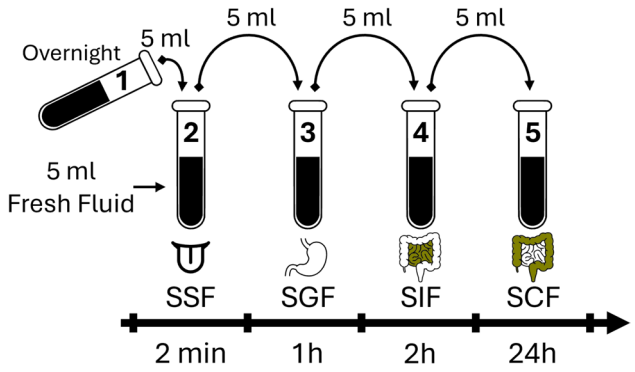

Fig. 1 Schematic workflow in gastrointestinal tract simulation

for 24 h, 240 rpm. Samples of 20 µl were taken from each initial and final cell suspension of a given part of the tract, then serially diluted tenfold in 96-well plates and seeded onto SAB agar plates for CFU estimation. The difference in relative viability (ΔRV) was calculated as the ratio of CFU at the end to the CFU at the beginning of the incubation in a particular section of the gastrointestinal tract:

$$\triangle \mathrm{RV} = \left(\frac{\mathrm{CFU}}{\mathrm{CFU}_{0\,\mathrm{h}}} - 1 \right)$$

A progressive twofold dilution was included in the CFU calculation due to the transfer of the yeast suspension to subsequent liquids.

Yeast Adhesion to the Gastrointestinal Mimicking Surface

Adhesion to the mucin was performed in a 24-well plate based on the method published in [20] with some modifications. First, 500 µl of sterile mucin (Merck, Germany) solution (10 mg/ml) in PBS (VWR, USA) was added to each well. Plates were incubated at 4 °C overnight to let mucin adhere to the bottom of the well. Each well was gently washed with 1 ml of sterile PBS the next day. Then, 500 µl of sterile BSA solution (20 mg/ml, Merck, Germany) was added to each well, and the plate was incubated at 4 °C for 4 h. Next, each well was gently washed with 1 ml PBS. Simultaneously, 1 ml of overnight WUT3, WUT151, or SB culture (in 3 biological repeats) was centrifugated (6000 × *g*, 10 min, 4 °C), washed with sterile PBS, and finally suspended in 10 ml of PBS, achieving a 10 × dilution of the initial cell suspension. Subsequently, 500 µl of cell suspension was added to each well covered with mucin and BSA. The plates were incubated for 1.5 h at 37 °C. Thereafter, wells were washed twice with 1 ml of PBS to remove unattached yeast cells. Then, 500 µl of Trypsin/EDTA (0.25%) was added, and the plate was incubated at 37 °C for 2–3 min. Initial yeast suspensions and yeasts detached after trypsinization were collected for microcultures to count the CFU.

Table 2 Cell lines used in this research. *NA*, not applicable

Cell line	Type	Passage	Cells/well
HT-29	Cancer	14	2.5×10^5
HCT-116	Cancer	15	2.5×10^5
CaCo-2	Cancer	4	2.5×10^5
CCD-18 Co	Normal	11	1.25×10^5
CCD-841 CoN[a]	Normal	22	NA

[a]CCD-841 CoN was used only for the toxicity determination

Adhesion to the cell lines was performed in a 24-well plate using the ATCC cell lines provided by LGC Standards (Table 2). Normal cells were grown in MEM (cat. no. 392–0423, VWR, USA) with 10% FBS (Columbia origin, EURx, Poland), 1% Pen/Strep (Merck, Germany), 2 mM L-Glutamine (Merck, Germany); HT-29 and HCT-116 in McCoy's 5 A (cat. no. M4892, Merck, Germany) with 10% FBS, 1% Pen/Strep; Caco-2 in EMEM (cat. no. 30–2003, ATCC, USA) with 20% FBS, 1% Pen/Strep; at 37 °C, 5% CO_2. Cells were subcultured using Trypsin–EDTA (0.25%, Thermofisher, USA) and diluted in growth medium to 5×10^5 cells/ml for cancer cells or 2.5×10^5 cells/ml for normal cells. Then, 500 µl of human cell suspension was added to the 24-well plate in 3 independent repeats. Plates were then incubated at 37 °C, 5% CO_2 for 72 h. After incubation, the confluence of cells reached 90–100%. Following the steps described above in mucin adhesion, a 10 × dilution of overnight yeast suspensions was prepared (about 2×10^7 cells/ml). A total of 500 µl of yeast suspension was added to each well, and the plates were incubated at 37 °C, 5% CO_2 for 1.5 h. Initial yeast suspensions were collected for microcultures. Thereafter, wells were washed twice with 1 ml of PBS to remove unattached yeast cells. Then, 500 µl of Trypsin/EDTA (0.25%) was added, and the plate was incubated at 37 °C for 2–3 min. Subsequently, ten-fold serial dilutions were prepared and seeded on the SAB or YPD agar plates to estimate the CFU number. Adhesion was calculated as the ratio of CFU after trypsinization to the CFU in the initial yeast suspension.

Autoaggregation and *S. cerevisiae* Sedimentation Model

A total of 2 ml of overnight yeast cultures were centrifugated (4000 × *g*, 5 min) and washed twice with PBS. Then, the cell pellet was suspended in 2 ml of PBS, and initial OD600 was measured (A_0). Cell suspensions were incubated in spectrophotometric cuvettes in RT without shaking, and

OD600 was measured (A_T) every 20 min for 300 min. The autoaggregation rate was calculated as the A_T and A_0 ratio.

The detailed derivation of the sedimentation model of yeast cells can be found in Supp. Data 2. The following formula was obtained, describing the sedimentation of cells:

$$A_{rel} = \exp(-\psi \bullet t)$$

where A_{rel} is the relative absorbance (A_T/A_0), ψ is a constant characteristic for the fluid and cells, and t is the time.

Hydrophobicity

Hydrophobicity was determined according to the protocol proposed by Fu et al. with modifications [21]. Yeast suspension was prepared as described in the autoaggregation protocol, and initial OD600 was measured (A_0). Then, 1 ml of cell suspension was transferred to the centrifuge flask, and 200 µl of chloroform was added, mixed for 15 min, and left at RT until clear phase separation. Then, the top water layer was gently mixed by pipetting to suspend cells that sedimented on the surface of the chloroform, and OD600 was measured (A_T). Yeast hydrophobicity (H_P) was calculated with the formula:

$$H_P = \left(1 - \frac{A_T}{A_0}\right) \bullet 100\%$$

Drug Resistance

Drug resistance of yeast strains was tested against the following 6 antibiotics: amphotericin B (AMB, 10 mg/ml, BioShop, Canada), geneticin G-418 (GEN, 20 mg/ml, Merck, Germany), tetracycline (TET, 10 mg/ml in 50% ethanol, Merck, Germany), ampicillin (AMP, 100 mg/ml, BioShop, Canada), chloramphenicol (CHL, 10 mg/ml in 50% ethanol, Merck, Germany), and streptomycin (STR, 20 mg/ml, Bioshop, Canada). *Candida albicans* ATCC10231 and *Escherichia coli* ATCC8739 were used as controls. Agar plates (YPD for yeast, LB for bacteria) were inoculated with 100 µl of yeasts or control strains overnight cultures. Then, sterile paper discs were placed on the agar and soaked with 5 µl of antibiotic solution. Agar plates were incubated at 37 °C bottom down for 24 h. Finally, the diameter of growth reduction was measured. All experiments were carried out in 3 independent biological and 3 technical repeats.

Antioxidant Activity

The antioxidant properties of yeasts were determined by the ability to reduce the free radicals content of 1,1-diphenyl-2-picrylhydrazyl (DPPH, Merck, Germany). A total of 1 ml of overnight yeast cultures in SAB were centrifugated (5000 × *g*, 5 min), washed twice, and suspended in 1 ml of sterile RF (0.9% sodium chloride). OD600 of the initial suspension was measured. A total of 500 µl of 0.2 mM (78.8 mg/l; 0.79%(w/v)) DPPH (Merck, Germany) solution in methanol was added to the sterile centrifugation flasks. Then, 500 µl of cell suspension or control was added, mixed, and incubated for 30 min in the dark. After incubation, samples were centrifugated to remove cells (5000 × *g*, 5 min), and 200 µl of supernatant was transferred to the 96-well plate. Absorbance was read using an automatic plate reader for $\lambda = 517$ nm. Antioxidation potential was calculated using the formula:

$$A_{OX} = \frac{A_{\text{blank}} - A_{\text{test}}}{A_{\text{blank}}} \bullet 100\%$$

where A_{OX} is the antioxidant potential, A_{test} is test wells absorbance, and A_{blank} is blank wells absorbance.

Antagonistic Properties

The experiment was performed with the use of pathogenic bacteria: *S. aureus* ATCC6538 (SA), *Bacillus subtilis* ATCC6633 (BS), *E. coli* ATCC8739 (EC), *Pseudomonas aeruginosa* ATCC9027 (PA), *Salmonella* Typhimurium ATCC14028 (ST), and pathogenic yeasts: *C. albicans* ATCC10231 (CA), *Candida tropicalis* WUT5 (CT), *Clavispora lusitaniae* WUT17 (CL). CT and CL were provided by the WUT Yeast Collection, Poland.

Bacteria were cultured in LB and yeast in YPD media overnight. Then, solid yeast cultures were prepared. First, 700 ml of MHB supplemented with $2\%_{w/v}$ glucose and $1\%_{w/v}$ agar was autoclaved and split by 70 ml into sterile flasks. Flasks were then chilled and inoculated with 700 µl of overnight WUT3, WUT151, or SB cultures, leaving one flask uninoculated as a pathogen control. The medium was quickly spilled into 3 plates and left to solidify. Then, 5 µl of overnight pathogen culture was dropped on the agar surface. When drops were absorbed into the agar, plates were incubated at 37 °C. Finally, the difference in pathogen growth diameter was measured.

Three pathogenic molds were used: *Aspergillus niger* ATCC 16404 (AN), *Fusarium oxysporum* MF 5 (FO), and *Fusarium sambucinum* MF 1 (FS). FO and FS were provided by the IHAR-PIB collection of Plant Breeding and Acclimatization Institute, Młochów, Poland. Solid yeast cultures were prepared following the abovementioned steps for the antibacterial test. Then, a small amount of pathogen spores was spotted inside the middle of the agar using a sterile needle. Plates were incubated at 30 °C for 72 h, and the diameter of the fungi was measured.

Growth inhibition was calculated using the formula:

$$I = \frac{d_{\text{control}} - d_{\text{test}}}{d_{\text{control}}} \bullet 100\%$$

where I is pathogen growth inhibition [%], and d_{test} and d_{control} are the diameters of pathogen growth [mm].

EVs Isolation and Characterization

Yeasts' EVs were isolated using a multistep filtration protocol, as previously described in [22]. First, 150 ml of SAB was inoculated with 3 ml of WUT3, WUT151, or SB overnight cultures and incubated for 20 h with shaking (220 rpm) at 37 °C. Next, cells were harvested by centrifugation (4500 × *g*, 10 min, 4 °C), and the supernatant was filtered on a 0.2 µm sterile PES vacuum filter (VWR, USA). Then, 15 ml portions of the filtrate were transferred to the 100 kDa regenerated cellulose centrifugal filters (Merck). The filtration was carried out centrifugating at 3200 × *g*, 8–20 min, 4 °C. After each filtration, concentrated EVs were pulled into the same centrifugal flask. When all EVs were filtered, EVs were rinsed twice in PBS and filtered on the same membrane. Isolated EVs were stored at − 80 °C.

Size distribution and EVs concentration were measured using nanoparticle tracking analysis (NTA, NanoSight Pro, Malvern Panalytical, UK) using NS Explorer ver. 1.1.0.6 software. Samples were diluted 1000 × (WUT151, SB) or 100 × (WUT3) in PBS. Analysis was performed using automatic camera and focus settings, with a 5 µl/min flow rate, capturing 10 videos of 750 frames each.

The morphology of EVs was analyzed by transmission electron microscopy (TEM) in the Laboratory of Electron Microscopy, which serves as an imaging core facility at the Nencki Institute of Experimental Biology (PAS) and is part of the infrastructure of the Polish Euro-BioImaging Node according to a previous publication [22]. A sample was adsorbed on a Formvar/carbon-coated copper grid (400 mesh, Ted Pella Inc., Redding, USA) for 20 min. The adsorbed EVs were then fixed with 1% (w/v) glutaraldehyde (Electron Microscopy Sciences, USA) for 5 min. The grids were then washed with distilled water 10 times for 1 min each and stained with a 2% (w/v) aqueous uranyl acetate solution (Serva, Germany) for 5 min in the dark. Finally, the grids were dried at room temperature for 24 h and examined using a JEM 1400 (JEOL Co., Japan). All incubations were performed at room temperature (RT).

EVs Proteins Identification

Mass spectrometry (MS) analysis was performed at the Mass Spectrometry Laboratory at the Institute of Biochemistry and Biophysics PAS, according to a previous publication [22]. After drying the isolated yeast EVs, the pellet was resuspended in 100 µl of 100 mM ammonium bicarbonate buffer containing 2% SDS and 10 mM tris(2-carboxyethyl)phosphine (TCEP). Samples were boiled at 95 °C (15 min), vortexed (15 min), and sonicated (15 min). To block reduced cysteines, 2 M methyl methanethiosulfonate (MMTS) was added to a final concentration of 20 mM, and the samples were incubated at room temperature for 10 min.

Protein samples were processed using the single-pot solid-phase-enhanced sample preparation (SP3) method with some modifications [23]. The magnetic beads mix was prepared by combining equal parts of Sera-Mag Carboxyl hydrophilic and hydrophobic particles (65152105050250 and 45152105050250, Cytiva). After washing with MS-grade water three times, the beads mix was resuspended to a working concentration of 10 µg/µl. A total of 80 µl of the prepared bead mix was added to each sample, along with phase B (0.1% formic acid in acetonitrile) to a final concentration of 80%. Proteins bound to beads were washed four times with 80% ethanol and once with acetonitrile. The dried resin was suspended in 150 µl of 100 mM ammonium bicarbonate buffer with 2 µg of trypsin (Promega). The digestion was performed overnight at 37 °C. After digestion, peptide solutions were transferred to new tubes, and the resin was washed twice with 40 µl 1% DMSO in water and 60 µl water. Pooled peptide eluates were acidified to a concentration of 0.1% formic acid.

Peptides were analyzed using an LC–MS system consisting of an Evosep One (Evosep Biosystems, Denmark) coupled with an Orbitrap Exploris 480 mass spectrometer (Thermo Fisher Scientific, USA). Half of the peptides were loaded onto disposable Evotip Pure C18 trap columns (Evosep Biosystems, Denmark) for each sample, according to the manufacturer's instructions. The bound peptides were washed three times with 100 µl and then covered with 300 µl of solvent A (0.1% formic acid in water).

Chromatographic separation was achieved using a preformed 88-min gradient on an analytical column (ReproSil Saphir C18, 1.5 µm beads, 150 µm ID, 15 cm length, Bruker Daltonics, USA) at a 220 nl/min flow rate. Data acquisition was conducted in positive ion mode using a data-dependent acquisition method with the following settings: MS1 scans were obtained at a resolution of 60,000, with a normalized AGC target of 300%, an automatic maximum injection time, and a scan range of 300 to 1600 m/z. MS2 scans were carried out at a resolution of 15,000, with a standard normalized AGC target and automatic maximum injection time. The top 40 precursor ions were selected for MS/MS analysis within an isolation window of 1.6 m/z. A dynamic exclusion period of 20 s was applied, with a mass tolerance of ± 10 ppm and a precursor intensity threshold of 5×10^3. Fragmentation was performed using higher-energy collisional dissociation (HCD) with a normalized collision energy of 30%. The source parameters included a spray voltage of 2.1

kV, a funnel RF level of 40, and a heated capillary temperature set at 275 °C.

Raw data from MS analysis were pre-processed with the Mascot Distiller software (v. 2.4.2.0; Matrix Science), and then obtained peptide masses and fragmentation spectra were matched to the Saccharomyces Genome Database (SGD, 2021, 6716 sequences; 3,018,905 residues) and cRAP (115 sequences; 38,188 residues) using the Mascot search engine (Mascot Daemon v. 2.4.0, Mascot Server v. 2.4.1, and Matrix Science). To reduce mass errors, the peptide and fragment mass tolerance settings were established separately for individual LC–MS/MS runs after a measured mass recalibration, resulting in values of 5 ppm for parent and 0.01 Da for fragment ions. The rest of the search parameters were as follows: enzyme specificity was set to trypsin, methylation of cysteine was set as fixed, oxidation of methionine was set as a variable modification, two missed cleavages were allowed, the protein mass was left as unrestricted, and mass values were set as monoisotopic. The mass calibration and data filtering were carried out with MScan software (http://proteom.ibb.waw.pl/mscan/). The Decoy Mascot functionality was used to keep FDR for peptide identifications below 1%. All peptides with q-values > 0.01 and proteins identified by a subset of peptides from another protein were removed from further analysis. The list of identified proteins was exported to Excel MS software. Next, data was cleaned by removing protein hits present only in one biological repeat and all queries with less than 3 peptides. Then, GO enrichment analysis was performed using ShinyGO 0.80 and Alliance Mine (access 23.07.2024). *S. cerevisiae* (taxonomy ID: 559,292) was set as the reference species. The analysis was performed using 4 pathway databases: KEGG, GO biological components, GO biological function, and SGD protein domain. The false discovery rate (FDR) cutoff was set to 0.05 and 2–5000 pathway size. Data were interpreted based on FDR, number of genes, and fold enrichment (FE).

The obtained proteomics data have been deposited to the ProteomeXchange Consortium via the PRIDE partner repository and are available via ProteomeXchange with dataset identifier PXD055073 (https://dx.doi.org/https://doi.org/10.6019/PXD055073). For more information on proteomic data, see Supp. Data 3.

EV Protein Marker Search

A search for EVs protein marker candidates was conducted on proteins shared among WUT3, WUT151, and SB. First, the peptide hits for each protein from 3 biological repeats of a given strain were summed up. Then, the data were sorted in ascending order for each strain, assuming that the quality of a biomarker candidate would depend on its relative frequency of peptide counts for a given protein. Still, the total number of peptide counts differed between strains. Therefore, categorizing by rank was applied using the formula below to make the results independent of the total number of peptide counts.

$$\text{Rang} = \text{No. of proteins} \bullet \frac{\text{No. of unique scores left}}{\text{Total no. of unique scores}}$$

For instance, among 179 shared proteins, SB had 61 uncial peptide hits (scores). The protein with the highest score (MET6) Rang $= 179 \bullet \frac{61}{61} \cong 179$. As the first score was unique, the second protein got Rang $= 179 \bullet \frac{60}{61} \cong 176$. If more than one protein has received the exact peptide hits, their ranks would remain the same. After ranking the results, the sum of ranks for each protein (among WUT3, WUT151, and SB) was calculated and arranged in descending order. This led to the final dataset, where proteins with higher ranks were assumed to be more appropriate candidates for EVs biomarker. Those proteins were then analyzed in terms of yeast specificity and associations with extracellular components.

EVs Cytotoxicity

The cell lines listed in Table 2 were transferred on 96 well plates at 5×10^3 cells (HT-29, HCT-116, CaCo-2) or 2.5×10^3 cells (CCD-18 Co, CCD-841 CoN) per well and incubated at 37 °C, 5% CO_2 for 24 h. Samples of the EVs were prepared at the end of the incubation period by dilution in a medium suitable for the cell line. Then, cells were washed with PBS, and EVs were added in 3 test concentrations: 10^2, 10^3, and 10^4 EVs per cell (5×10^5 – 5×10^7 EVs per well). 5% DMSO was added as the positive control, and pure growth medium as the negative control. Plates were incubated at 37 °C, 5% CO_2 for the next 24 h. Then, metabolic activity was examined using an MTT assay. Wells were washed with PBS, and 100 µl of 0.5 mg/ml (HT-29, HCT-116, CaCo-2) or 1.0 mg/ml (CCD-18 Co) MTT solution in a suitable cell medium was added. Plates were incubated in the dark at 37 °C, 5% CO_2 for 2 h. Then, the wells were washed with PBS. A total of 50 µl of DMSO was added to dissolve formazan crystals, and plates were incubated in the dark at RT, 240 rpm for 10 min. Absorbance was measured at 570 nm using a plate reader (Synergy H4 Hybrid Reader, BioTek). Viability was calculated using the formula:

$$V = \frac{A_T - A_B}{A_C - A_B} \bullet 100\%$$

where A_T is absorbance of test wells, A_B is blank, and A_C is the absorbance of negative control wells.

Table 3 Metabolic parameters of WUT3, WUT151, and SB. *Gluc*., glucose; *Sucr.,* sucrose; *Galact*., galactose; *Malt*., maltose; *Glyc*., glycerol; *EtOH*, ethanol; +, growth; -, no growth; *w*, weak growth

Yeast strain	Carbon source assimilation						Enzymatic activity	
	Gluc	Sucr	Galact	Malt	Glyc	EtOH	Proteolytic	Hemolytic
WUT3	+	+	+	+	w	w	-	-
WUT151	+	+	+	-	-	-	-	-
SB	+	+	-	+	+	w	-	-

EVs Integration with Human Intestinal Cells In vitro

Microscopic observations were performed on microscopic slides with 8 well chambers for cell culture (Biologix, Germany). First, 400 µl of 3.125×10^6 cells/ml HT-29 or HCT-116 cell suspension was put on the slides and incubated at 37 °C, 5% CO_2 for 72 h. Then, EVs of WUT3, WUT151, and SB at the concentration of 2×10^{11} EVs/ml were stained with Nile Red according to the protocol in [22]. Cells on the slides were washed 3 times with 400 µl of PBS. Thereafter, 25 µl of stained EVs and 200 µl of PBS were transferred to the cells and incubated in the dark at 37 °C, 5% CO_2 for 15 min. Simultaneously, one well per cell line was treated with PBS, which underwent a staining procedure analogous to EVs as a negative control. After incubation, EVs or PBS were discarded, and cells were fixed with 4% PFA for 15 min at RT. Fixed cells were gently washed 2 times with 400 µl of PBS and stained with 300 nM DAPI (Thermofisher, USA) for 2 min. The fluid was removed from the wells, and the slides were enclosed with coverslips. Cells were observed using a Nikon Eclipse Ni fluorescence microscope, with Plan Fluor 60 ×/0.85 or 100 ×/1.30 oil lens, CFI 10 ×/22 ocular, blue (392/23 nm; 447/60 nm) or red (554/23 nm; 609/54 nm) fluorescent filters, and Nikon DS-Fi3 camera. Images were captured with NIS Elements DR ver. 5.30.04 software.

Data Analysis and Visualization

Unless otherwise indicated, the data were analyzed using Origin Pro 2021b software with an academic license. ANOVA analysis with the HSD Tukey post-hoc test was used to statistically compare means if the data were normally distributed (Shapiro–Wilk test) with homological variances (Brown-Forsythe test). If data did not meet the assumptions of ANOVA, the Kruskal–Wallis non-parametric test with Dunn's post hoc test was used instead. A standard 5% level of significance was used. Data were presented as mean ± standard error (SE) unless otherwise indicated. A one-sided t-test was used to compare data with a given threshold, e.g., ISO 10993–5:2009 toxicity criterion. The data visualization was carried out using the same software. In the graphs, strains were color-coded: WUT3 (blue), WUT151 (orange), and SB (green).

Results

WUT3 and WUT151 Show Similar or even Better Probiotic Properties than the Reference Strain CNCM I-745

Two strains of *S. cerevisiae*, WUT3 and WUT151, isolated from spontaneously fermented cow's milk, were compared for their physiological and probiotic properties with *S. cerevisiae* var. *boulardii* CNM I-745 (SB). Looking at the basic metabolic parameters, such as carbon substrate assimilation, some differences are visible between the strains (Table 3). In contrast to SB, the two WUT strains metabolize galactose. WUT151 does not grow on maltose, glycerol, and ethanol, whereas WUT3 and SB do. Both WUT strains, like the SB, lack the proteolytic and hemolytic activity expected of probiotic candidates.

Growth at 37 °C is an important characteristic of probiotics, so a closer look was taken at how the WUT yeasts perform at this temperature. Forty-eight-hour batch cultures were carried out, during which growth was monitored by measuring OD600, determining CFU/ml, and weighing dry biomass. In addition, microscopic observations were conducted to estimate the cell diameter and morphology. Based on certain parameters, such as maximum specific growth rate, generation time, and biomass production efficiency, it was noticed that the WUT strains achieved better scores than the reference SB strain (Fig. 2A). WUT151 displayed approximately 40% and 115% more biomass production than WUT3 and SB, respectively. What correlates also with the highest cell density (CFU/ml) and OD600 achieved by this yeast, $2.02 \pm 0.52 \times 10^7$ and 7.01 ± 0.73, respectively. Although the WUT3 strain reached a lower cell density (CFU/ml) than the others (Fig. 2B), its cells are larger (Fig. 2C), and this may translate into OD600 values that are similar to those of SB (5.51 ± 0.23 vs. 4.48 ± 0.32). Row biomass data are available in Table S1.

A key feature of probiotics is their resistance to harsh conditions in the digestive tract of humans and animals. Therefore, the yeast survival in simulated saliva, gastric, and intestine fluids was evaluated. The WUT3 and WUT151 strains maintained positive relative viability differences (ΔRV) in each tested gastrointestinal fluid, indicating that yeast concentration was always increasing. Conversely, the SB had ΔRV established at neutral

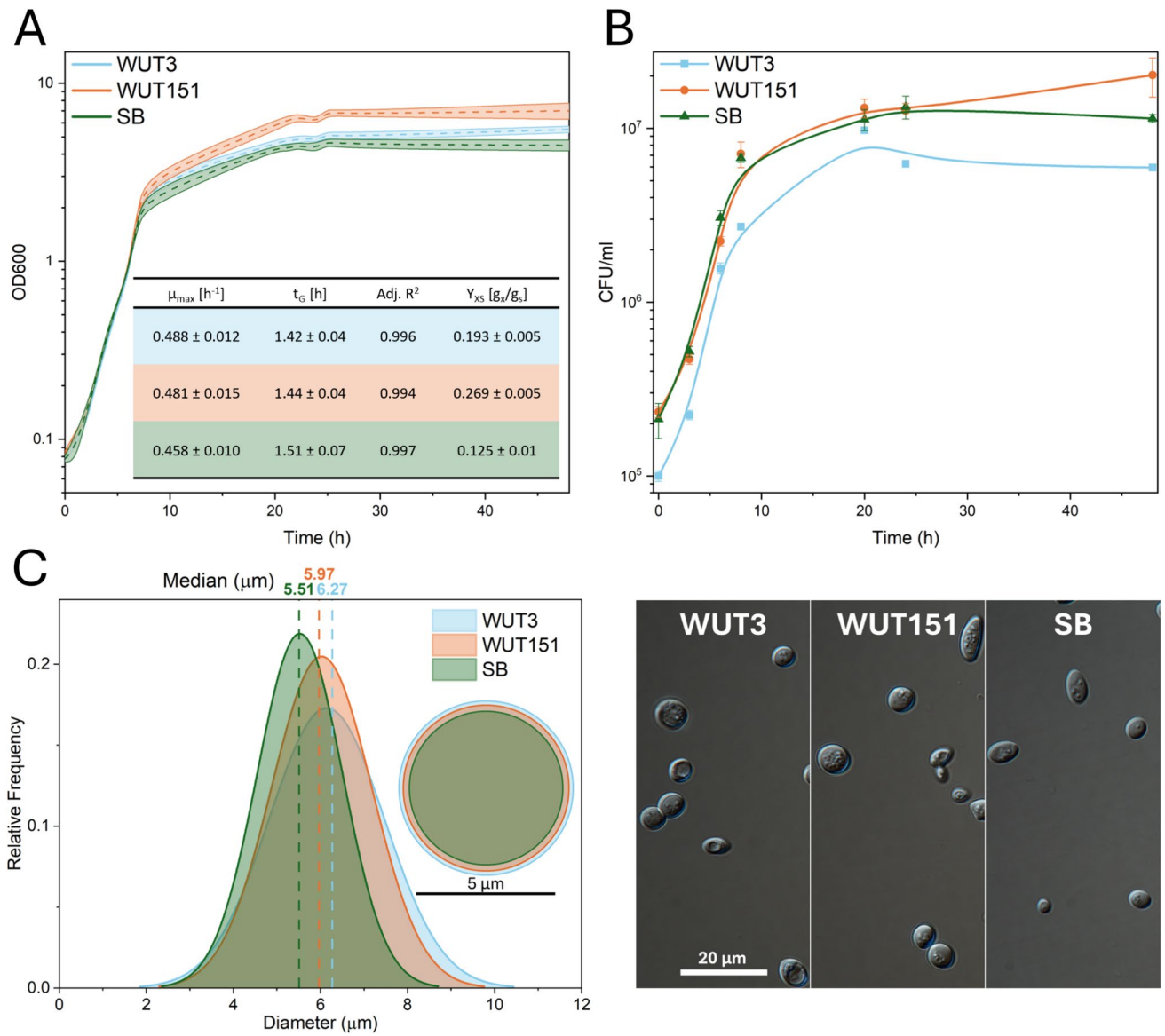

Fig. 2 Yeast growth characteristics at 37 °C. **A**, **B** Growth curves and parameters (μ_{max}, maximum specific growth rate; t_G, dabbling time; Adj. R^2, adjusted R^2 for linear approximation of the logarithmic phase; Y_{XS}, biomass/substrate coefficient). **C** Yeast cells diameter distribution at 20 h of culture: WUT3 [N = 885, (Q1, Q3) = (5.34, 7.03)], WUT151 [N = 503, (Q1, Q3) = (5.27, 6.78)], SB [N = 955, (Q1, Q3) = (4.89, 6.14)] and representative microscopic images (1000 × magnification)

levels, reaching one negative value of − 0.43 ± 0.09 in SIF. This shows that even if the simulated media did not reduce SB viability, it prevented cell growth, prolonging the lag phase. In each of the tested yeast strains, incubation in SCF resulted in intensive growth, which can be seen as the significantly higher ΔRV compared to the other media ($p < 0.05$). The absolute CFU/ml values in the middle of each segment in Fig. 3 prove that all tested yeast can survive the intermediate gastrointestinal segments and grow in the SCF for at least 24 h with the yeast CFU/ml increase.

The physical properties of the yeast were then assessed, namely adhesion to the inner intestinal surface, hydrophobicity, and auto-aggregation, which are also crucial for the longer residence of probiotics in the gastrointestinal tract. The study revealed that yeasts showed higher adhesion to the mucin layer than human cells ($p < 0.001$, Fig. 4A). Among the strains, WUT3 adhered the most efficiently (71.9% ± 7.8%), significantly more than WUT151 (57.8% ± 2.2%, $p < 0.05$) and *S. boulardii* (48.2% ± 1.5%, $p < 0.001$). At the same time, all yeasts displayed statistically the same adhesion to the intestinal cell ranging from 6.3% ± 1.6% to 11.3% ± 2.2%. Moreover, both WUT strains and SB showed low hydrophobicity, between 12.1% and 23.9% (Fig. 4B). The sedimentation data matched the

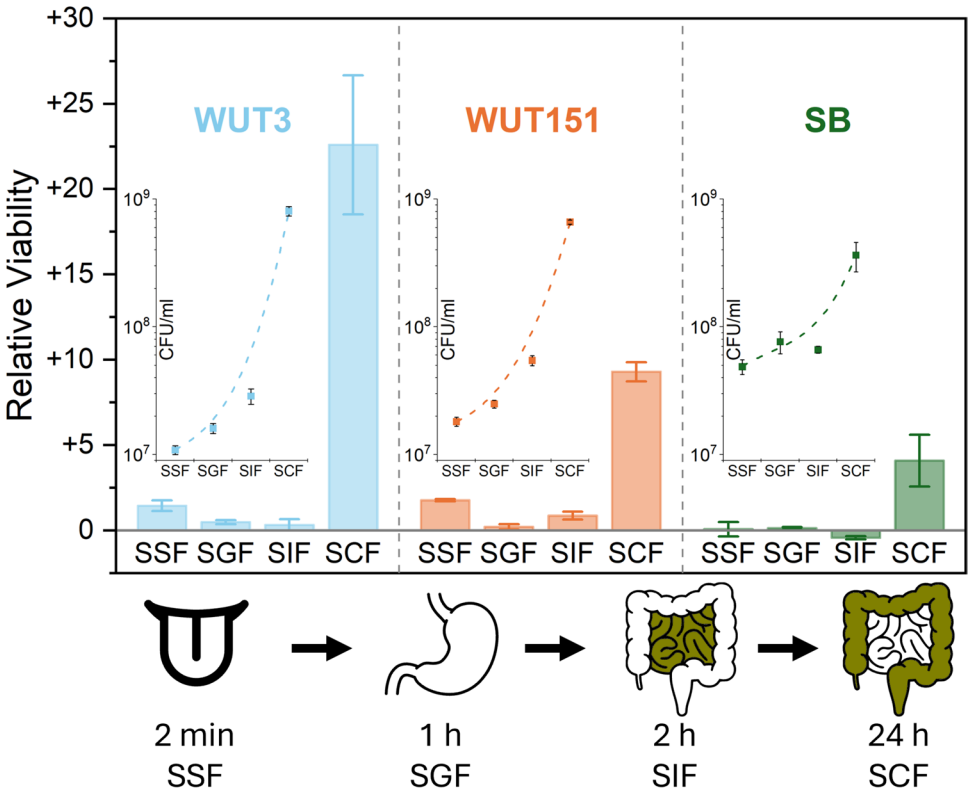

Fig. 3 Viability of yeasts in simulated gastrointestinal fluids. This figure illustrates that WUT3 and WUT151 exhibited reduced sensitivity to environmental stress compared to the SB. Bar plot – a difference in relative viability (ΔRV). Scatter plot – absolute CFU/ml values. The error bar indicates the standard error of the mean. SSF – simulated saliva fluid, SGF – simulated gastric fluid, SIF – simulated intestines fluid, SCF – simulated colon fluid

model predictions established for the purpose of this study (Fig. 4C). Modeling the process gives an advantage to compare autoaggregation speed, described as ψ parameter, which is a more precise approximation than comparing the times of t_{50} and t_{90}. Based on the ψ, WUT3 aggregated 23% ± 1.6% and 31% ± 2.3% faster than WUT151 and *S. boulardii*, respectively. For comparison, the difference was 30% and 44%, respectively, using the t_{50} or t_{90}.

Another characteristic shown by probiotics is their antioxidant activity, which benefits the host organism by reducing free radicals and reactive oxygen species. Therefore, WUT strains were also assessed by determining the percentage of DPPH radicals' reduction. All tested yeasts displayed similar antioxidation effects, comparable to the control HCOOH (Fig. 5). WUT3 reduced DPPH radicals' content by 77.3% ± 2.5%, WUT151 by 70.1% ± 1.5%, and SB by 65.3% ± 4.5%. HCOOH, as a potent reducing agent, neutralized 65.4% ± 0.8% of free DPPH radicals.

Antimicrobial activity is crucial since the presence of the probiotic strain should limit the spread and development of pathogens. To accomplish this, a series of tests were conducted against pathogenic bacteria, yeasts, and molds. Tested WUT strains showed limited properties to inhibit the growth of *Candida* sp. (Fig. 6A), and the highest inhibition was observed for WUT3, yet not exceeding 20%. Much higher antimicrobial properties were observed against the bacteria, especially *S. aureus* and *P. aeruginosa*. However, both WUT strains and SB displayed the strongest antagonism towards molds. The growth of *F. sambucinum* was totally stopped by all tested yeast strains. WUT3 almost completely prevented *A. niger* growth, while other yeasts showed approximately 80% inhibition. WUT3 and WUT151 inhibited the growth of *F. oxysporum* over 10% more than SB ($p < 0.05$).

It is also desirable that probiotics exhibit drug resistance to the standard antibiotics so that they can be used simultaneously with antibiotic therapy. On the other hand, some drugs must break that resistance to control probiotic growth. Of all tested antibiotics, only amphotericin B inhibited the growth of the yeasts. The WUT strains, as well as SB, were resistant to antibiotics routinely used for bacterial infection treatment: geneticin, tetracycline, ampicillin, chloramphenicol, and streptomycin (Fig. S1).

EVs Characterization

A growing number of studies indicate that microorganisms can affect human cells by secreting extracellular vesicles (EVs) [14, 16, 24]. Therefore, this report also addresses this issue. Firstly, EVs were isolated from liquid cultures of WUT and SB strains in the SAB medium and then physically characterized. Bilayer nanoparticles observed in TEM images proved successful EVs isolation from yeast cultures (Fig. 7A). Size distribution and EV concentration

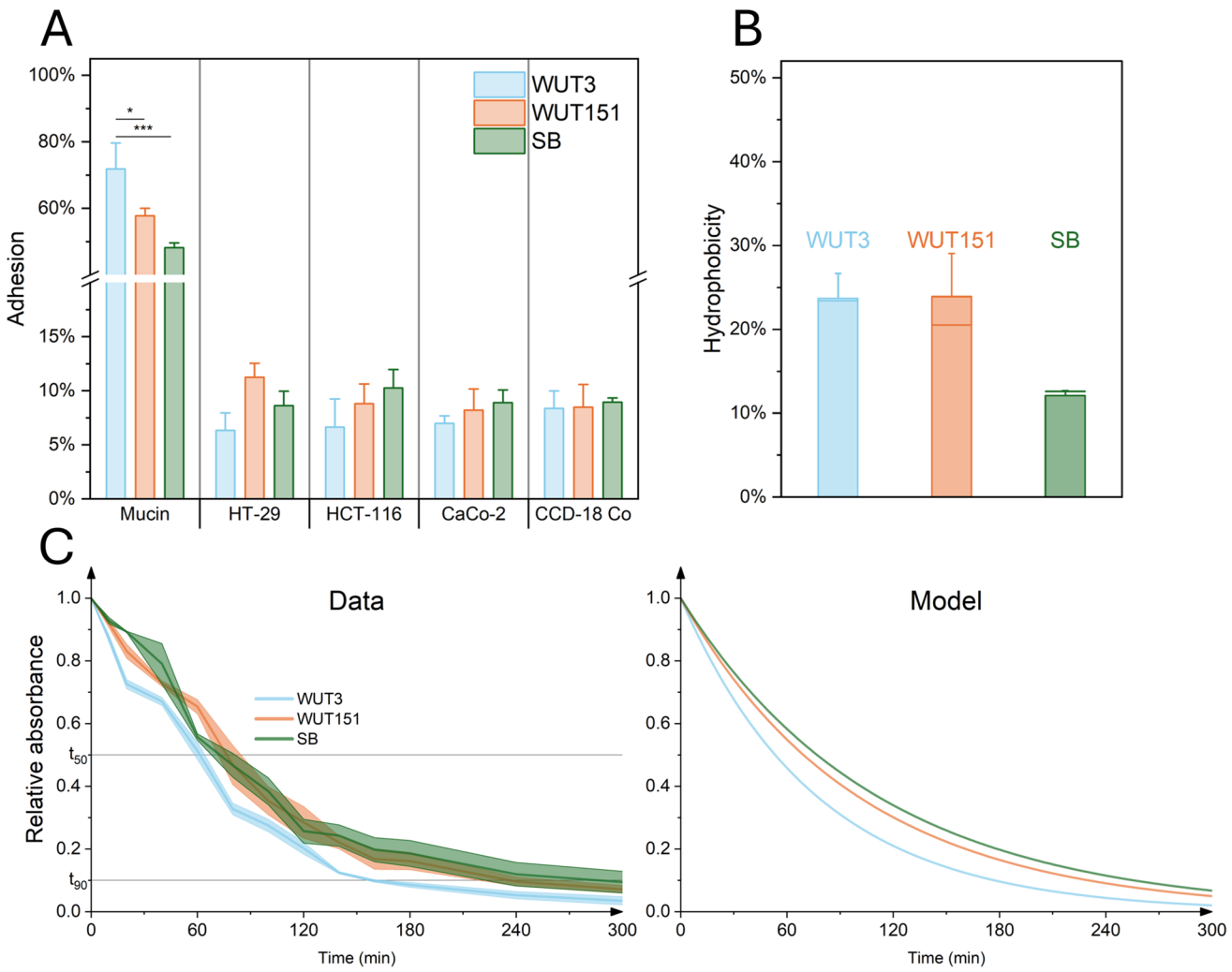

Parameter	WUT3	WUT151	SB
t_{50} (min)	53.32 ± 1.88	69.31 ± 2.44	77.02 ± 3.14
t_{90} (min)	177.12 ± 6.23	230.26 ± 8.11	255.84 ± 10.44
ψ (s^{-1})	0.013	0.01	0.009
SE	3.52%	3.52%	4.08%
R^2	0.9896	0.9887	0.9841

Fig. 4 Physical probiotic properties of yeast. As depicted in the figure, WUT3 and WUT151 showed no worse performance than SB. **A** Adhesion to the biological surface (mucin or human intestinal cells). **B** Hydrophobicity (line indicates median). **C** Autoaggregation and sedimentation. Error bars indicate standard error. *$p < 0.05$, ***$p < 0.001$. t50, t90—time needed for sedimentation of 50% and 90% of cells

were determined by Nanoparticle Tracking Analysis (NTA) (Fig. 7B). This revealed that the WUT151 strain produced EVs with the largest mode diameters (165.5 ± 2.7 nm), significantly exceeding those from WUT3 and SB vesicles (125.5 ± 4.4 nm, $p < 0.001$ and 141.8 ± 4.7 nm, $p < 0.05$). Based on the concentration of EVs in the samples, also assessed via NTA, the efficiency of vesicle isolation was estimated to be $4.35 \pm 2.51 \times 10^9$, $3.72 \pm 0.98 \times 10^9$, and $3.47 \pm 0.55 \times 10^9$ EVs per 1 ml culture of WUT3, WUT151, and SB, respectively.

Moreover, knowing the number of viable yeast cells in each culture (CFU/ml), it was possible to determine that a single cell of WUT3, WUT151, and SB released at least 119 ± 40, 57 ± 16, and 232 ± 53 EVs, accordingly.

Next, the toxicity of yeast EVs against human intestinal cell lines, three cancerous and two normal, was investigated.

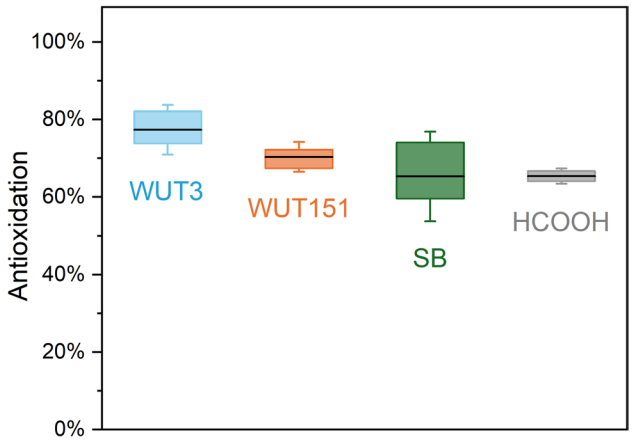

Fig. 5 Ability of yeasts to reduce the free radical content of 1,1-diphenyl-2-picrylhydrazyl (DPPH). Tested strains reduced free radicals content similar to the organic reductant–formic acid HCOOH (used as positive control). The bar indicates a 25–75 percentile range, the error bar indicates the SE of the mean, and the line marks the mean

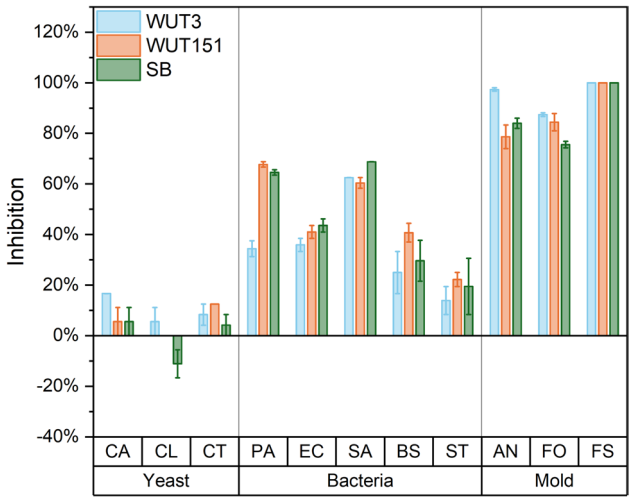

Fig. 6 Yeast antimicrobial properties against pathogens. The presented graph shows that WUT3 and WUT151 reduced pathogen growth similar to the SB. AN, *Aspergillus niger*; BS, *Bacillus subtilis*; CA, *Candida albicans*; CL, *Clavispora lusitaniae*; CT, *Candida tropicalis*; EC, *Esherichia coli*; FO, *Fusarium oxysporum*; FS, *Fusarium sambucinum*; PA, *Pseudomonas aeruginosa*; SA, *Staphylococcus aureus*; ST, *Salmonella* Typhimurium. Mean ± SE

The IC_{50} value was not reached in any of the tested variants. Based on a one-sided t-test, the 30% toxicity threshold (according to EN ISO 10993–5:2009) was only exceeded in studies on the cancer HT-29 cell line (Fig. 8). In the highest EVs/cell concentration, WUT151 EVs (45.0% ± 3.3%) and SB EVs (44.6% ± 3.8%) displayed greater toxicity to HT-29 cells than WUT3 EVs (36.8% ± 0.6%, $p < 0.001$). A negative correlation between EV concentration and cell viability was only observed when CaCo-2 and CCD-841 CoN cells were treated with SB and WUT3 EVs, respectively. Regarding ISO10993-5:2009 restrictions, none of the EVs were toxic against normal cell lines (CCD-18 Co and CCD-841 CoN).

EVs Integration with Intestinal Cells In vitro

Recently, it has been shown that SB EVs can integrate with human cells in vitro [22]. Thus, to elucidate whether it is a common feature for *S. cerevisiae* EVs, the next studies aimed to track EVs–cell interactions. Therefore, EVs of WUT3, WUT151, and SB were stained with a lipophilic cell membrane stain, Nile Red, and then incubated with the HT-29 and HCT-116 cells (Fig. 9). A red fluorescence on the surface of the cells indicated the interaction of the EVs and cell membranes. Treatment of both cell lines with all tested yeast EVs resulted in the emission of red fluorescence. However, the signal seemed to be weaker in cells incubated with WUT3 EVs. This may suggest that EVs from the WUT3 strain either interact less efficiently with human cells or do not incorporate Nile Red as efficiently as EVs from the WUT151 and SB strains. Nevertheless, the employed observation technique can only facilitate qualitative analysis, so further studies are needed to verify these findings.

Protein Profile of the Yeast EVs

Finally, proteomic analysis of the EVs cargo was carried out to provide information on the most common proteins. This analysis can also be used to explore the mechanisms of the formation and release of EVs by yeast. The three main factors that were analyzed were *proteins*, indicating how many proteins are categorized to the given group; *FE* (fold enrichment), indicating how protein population is over or under-represented compared to the reference strain; and *FDR* (false discovery rate), indicating how many proteins were falsely assigned to a particular group; FDR $< 10^{-5}$ is considerate as statistically significant.

With the use of MS analysis, it was possible to identify proteins present in the EV probes of WUT3 (196), WUT151 (1246), and SB (887). Tested strains shared 179 proteins, which were the base for the GO analysis (Fig. 10A). Almost all previously reported proteins from SB EVs (> 98%) were also present in this study (Fig. 10B) [22]. Entire data sets of proteomic analysis are collected in the supplementary_data_2.xlsx file, labeled as "Supplementary File" in the text below.

The proteomic analysis began with cellular component gene ontology enrichment (Fig. 10C). Of the 179 shared proteins, 92 (~ 50%) were from the cytosol (FE = 1.4, FDR $< 10^{-14}$). At first glance, not much, as only 40 proteins (~ 20%) were from the extracellular region (FE = 11.6, FDR $< 10^{-29}$). However, that represents 30% of all proteins

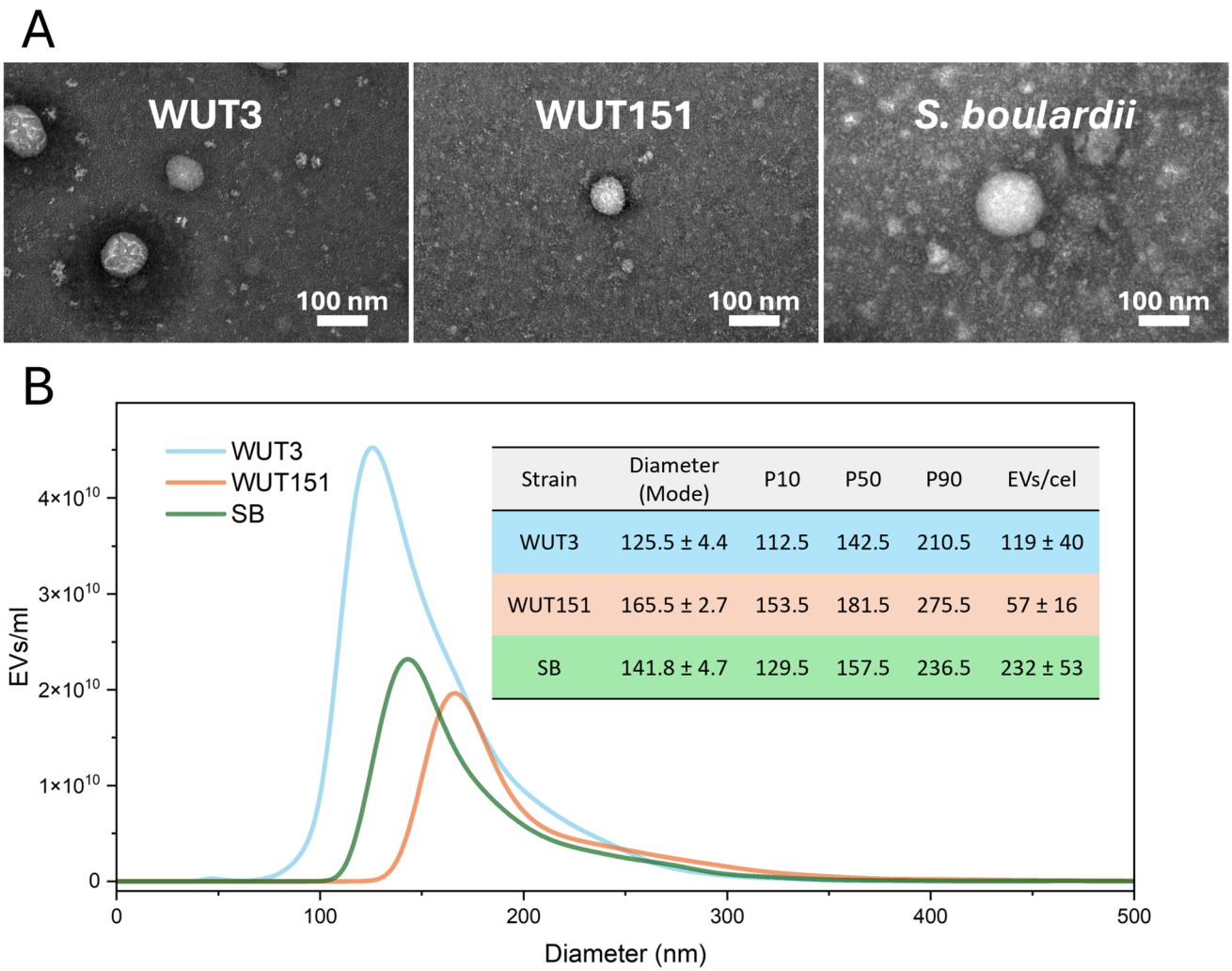

Strain	Diameter (Mode)	P10	P50	P90	EVs/cel
WUT3	125.5 ± 4.4	112.5	142.5	210.5	119 ± 40
WUT151	165.5 ± 2.7	153.5	181.5	275.5	57 ± 16
SB	141.8 ± 4.7	129.5	157.5	236.5	232 ± 53

Fig. 7 Characterization of EVs isolated from the WUT3, WUT151, and SB liquid culture. **A** TEM images of EVs. **B** EVs diameter distribution from NTA. Data in the table: mode (± SE), P10—10 th percentile, P50—median, P90—90 th percentile of EVs diameter (nm), and mean number of EVs per cell (± SE)

associated with this GO term, making it the most covered group in the analysis with very high FE. Combined with high FE for external encapsulating structure (FE = 8.7, FDR $< 10^{-22}$), it is reasonable to claim that proteins of this type are overrepresented in the EVs samples. About 43 proteins (24%) were related to the plasma membrane (FE = 2.6, FDR $< 10^{-7}$), the main component of the EVs surface. Another indication that EVs are extracellular structures is the extraordinary increase in the presence of proteins on the cell surface (FE = 19, FDR $< 10^{-15}$) and the external side of the plasma membrane categories (FE = 17, FDR $< 10^{-5}$) (Supplementary File).

Then, the GO molecular process (Fig. 10D) and the KEGG database (Fig. 10E) were screened to find enrichment in metabolism. Almost 35% ($N = 62$) of the proteins were engaged in some metabolic pathways (FE = 2.9, FDR $< 10^{-13}$). Pentose phosphate and glycolysis/glucogenesis were recognized as the most enriched pathways (FE > 8.9, FDR $< 10^{-4}$). In addition to the presented analysis, we were able to identify some ribosome subunits (FE = 6.3, FDR $< 10^{-12}$) and proteasome 20S core particles (FE = 5.5, FDR $< 10^{-2}$).

Regarding GO molecular functions (Fig. 10F), catalytic (FE = 1.9, FDR $< 10^{-15}$) and binding (FE = 1.3, FDR $< 10^{-3}$) activities were prominent, represented by 121 (68%) and 131 (73%) of shared proteins, respectively. Catalytic activity is more certain due to the lower FDR. Exploring the catalytic activity, the highest fold enrichment was observed for glucan endo-1,3-beta-D-glucosidase activity (FE > 30, FDR $< 10^{-5}$). In addition, hydrolase activity acting on glycosyl bonds (FE = 8.5, FDR $< 10^{-7}$) and glucosidase activity (FE = 9.8, FDR $< 10^{-4}$), more general categories, were also significantly overrepresented (Supplementary File). This may relate to the great enrichment of NAD + and NADP

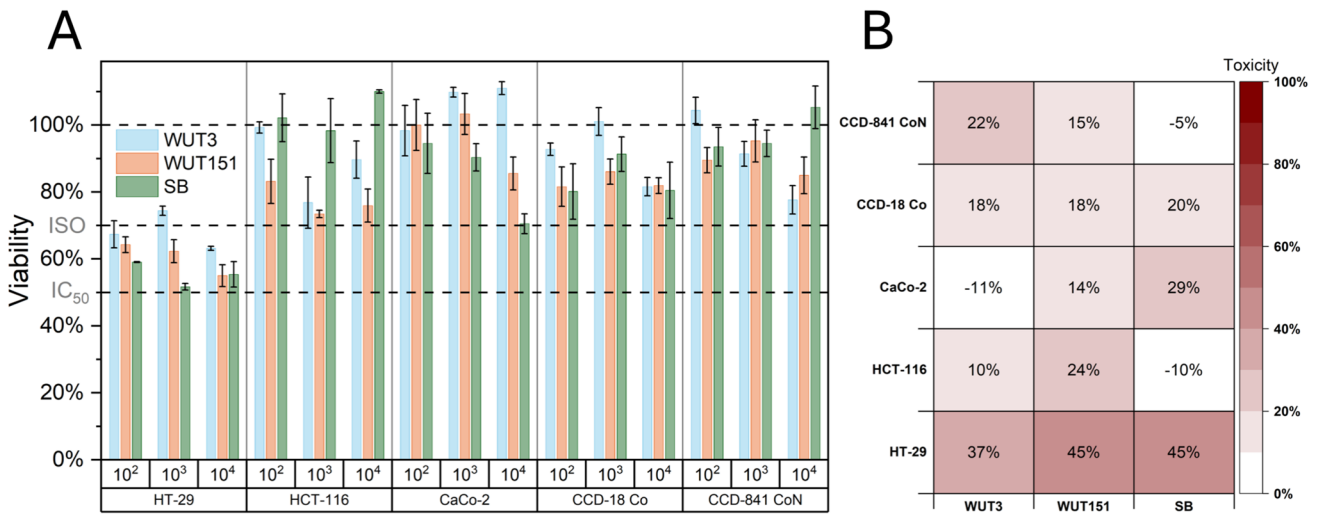

Fig. 8 Toxicity of yeasts' EVs against cancer (HT-29, HCT-116, CaCo-2) and normal (CCD-18 Co, CCD-841 CoN) cell lines. As depicted in the figure, EVs were not toxic against normal human cells. **A** Complete cell viability data, EVs concentration in 10^2–10^4 EVs/cell range, mean ± SE. The ISO marker shows a 30% toxicity threshold according to EN ISO 10993–5:2009. **B** Heat map of mean toxicity for 10^4 EVs/cell

+ dehydrogenases, enzymes of the glycolysis pathway. Peptidases ($N = 12$) and endopeptidases ($N = 9$) were the second most prevalent enzymes in the samples. Threonine and aspartic-type enzymes reached FE > 10, indicating their significant overrepresentation. Referring to previous results, it is worth noting that more than eightfold enrichment was detected for antioxidation activity (FDR $< 10^{-4}$).

Protein domain enrichment analysis was performed using SGD analysis tools and the STRING database. Of the 179 shared genes, 6 protein domains were significantly overrepresented. From those, one domain (PTHR16631) was related to the beta-glucan modifying enzymes (FDR < 0.05). Other domains were related to the metabolic pathways, in particular, 4 domains taking part in glycolysis (glycosidases: G3DSA:3.20.20.80, PS00587, SSF51445; G3P dehydrogenases: SSF55347) and one domain from amino acid biosynthesis (reductases: G3DSA:3.30.360.10).

Data from protein identification was also used to find reasonable *S. cerevisiae* EVs biomarker candidates. Normalized peptide counts from the MS were used to indicate a given protein's prevalence. Normalization was necessary to make the counts independent of the total number of proteins, which vary between strains. This approach allows to rank the proteins from the 3 strains in order from most frequently identified to least (Fig. 11). Proteins with the top 10 highest scores appeared to be non-specific for yeast or associated with yeast basic metabolism rather than the extracellular region. Therefore, lower-score proteins were further analyzed, verifying the specificity and connection to the extracellular region. Among these proteins, endo-beta-1,3-glucanase (Bgl2, YGR282 C) is abundant. Bgl2 is involved in cell wall maintenance and remodeling, possibly enabling EVs to cross that barrier. It is specific for yeast, as it involves a cell wall absent in human cells. Given the above, Bgl2 seems to be a promising *S. cerevisiae* EVs biomarker candidate.

Discussion

This study aimed to evaluate the probiotic properties of two *S. cerevisiae* strains, WUT3 and WUT151, isolated from Turkish and Kyrgyz fermented milk and to characterize their extracellular vesicles (EVs). All studies were conducted in parallel with a commercial probiotic—*S. cerevisiae var. boulardii* CNCM I-745. First, the physiological and growth parameters have been established. Neither WUT strain revealed hemolytic activity, which is consistent with other reports on *S. cerevisiae* and allows them to be considered safe for the human body [7, 27, 30]. The cultures of the WUT151 strain reached a higher final OD600 value than SB in the SAB medium at 37 °C with a similar number of CFU/ml in the stationary phase. *S. boulardii* has smaller cell diameters, distracting light less efficiently for the same cells' concentration, leading to decreased optical density, which explains the obtained results. Moreover, WUT151 obtained twice as much biomass while having CFU/ml values similar to those of SB, which supports this statement. WUT151 and WUT3 did not differ in size significantly. Although WUT3 produced more biomass than SB, the latter had more live cells in the stationary phase.

Probiotics are orally distributed, and before settling in the intestines, they must survive a harsh environment. Thus, survival in gastric and intestine fluids is a primary criterion for probiotic microorganisms [5]. This study shows that the yeast strains tested, WUT3 and WUT151, can survive a journey through an environment simulating the gastrointestinal tract in vitro for at least 2 min in saliva, 1 h in gastric fluid, 2 h in intestines fluid, and 24 h in colorectal fluid, similarly as a reference SB strain. However, a detailed analysis of the yeast growth revealed that *S. boulardii* entered the lag phase in the early stages of the digestive tract. At the same time, the WUT3 and WUT151 strains remained in the active growth phase. This means the SB underwent more stress under the influence of adverse environments. Some scientists have come to the opposite conclusion, indicating that *S. cerevisiae* is more sensitive to harsh gastrointestinal environments, leading to a 40% reduction in survival rate [25]. Over 10% CFU reduction in SGF and over 20% in SIF was also observed for *S. cerevisiae* I4 [26]. These suggest that the survival rate is strain-dependent. It is worth mentioning that, unlike in other reports, we have expanded the gastrointestinal tract studies with a complete simulation of the yeast passage through the digestive tract, including their settlement in the large intestine (SCF). After 24 h of incubation in SCF, yeasts could grow efficiently, increasing the number of living cells by about tenfold. In the case of the tested *S. cerevisiae* strains, we state that they display the same viability in gastrointestinal fluids as *S. boulardii*.

Adhesion to the intestinal tract is a significant parameter determining the application of a microorganism as a probiotic, since it has a substantial impact on intestinal colonization efficiency [27]. However, probiotics with too high adhesion properties could be administered less frequently to the patient, as they would stay too long in the intestine. The adhesion of yeast to the model human CaCo-2 cell line at levels 4–15% can be interpreted as suitable for probiotics [7]. On this basis, we can confirm that the WUT3 and WUT151 strains meet this requirement of probiotics. We have also conducted this research on other colorectal cancer and normal cell lines. The results were statistically identical to the CaCo-2 adhesion, validating our findings. Performing at least one experiment on the normal cell lines is essential, as they differ from cancer cells in phenotype and growth rate, making the adhesion surface different.

Autoaggregation and hydrophobicity directly impact yeast's ability to remain longer in the gastrointestinal tract [27]. Therefore, in parallel to adhesion tests, these additional parameters of potential probiotics have been determined. Starting with autoaggregation, *S. boulardii* had about 40 min lower t_{50} than previously reported in the literature [5]. This discrepancy may be due to the different methodology and measurement techniques. Fu et al. observed the same relationship, namely that *S. cerevisiae* ATCC9763, CICC1398, and ATCC9080 strains exhibit higher sedimentation speed at an early aggregation stage than *S. boulardii* (Jarrow Formulas, Vegan Saccharomyces Boulardii + MOS, food supplement) [21]. This is consistent with cell size, as the SB cells were the smallest. The hydrophobicity of some *S. boulardii* strains was reported at radically different levels, from 35% to almost 100% [5, 21, 27]. In the present study, the *S. boulardii* CNCM I-745 hydrophobicity was only 12.1% ± 1%, whereas it was almost twice as high for strains WUT3 and WUT151 of *S. cerevisiae*. Among the reports, there is a strong strain dependence in the hydrophobicity of *S. cerevisiae*. In the same trial, this parameter can reach 25% for one strain and levels exceeding 60% for another [21, 25]. Although *S. cerevisiae* WUT3 and WUT151 demonstrated higher hydrophobicity than SB, it was still almost three times lower than previously reported for *S. cerevisiae* ATCC strains. However, it should be kept in mind that culture conditions such as temperature, oxygenation, and medium composition directly impact the hydrophobicity, autoaggregation, and sedimentation of yeast cells. Therefore, as in our study, it is important to carry out such tests in parallel on reference probiotic strains, e.g., CNCM I-745, and not only to compare with other reports [21]. Moreover, we have proposed a good tool (see Materials and Methods Autoaggregation and S. cerevisiae Sedimentation Model) for comparing the sedimentation speed of multiple yeast strains. To the best of our knowledge, we are the first to develop an autoaggregation model for *S. cerevisiae* that fitted the data with an error of less than 2%.

Considering the above, *S. cerevisiae* strains WUT3 and WUT151 are more likely to survive longer in the harsh conditions that prevail in the environment of the human gastrointestinal tract than the probiotic CNCM I-745 strain. Besides, this study shows that WUT3 and WUT151 strains exhibit high antioxidation properties. This ability is profitable in reducing free radicals' content in the host environment (e.g., ROS). All tested yeast strains displayed antioxidation significantly above 50%, which is considered excellent [27]. Antioxidation of *S. cerevisiae var. boulardii* strains was reported to range widely from 40% [5, 27] up to 70% [21]. Our results at 65.3% ± 4.5% for the CNCM I-745 strain support outstanding SB's antioxidative properties. The WUT3 and WUT151 *S. cerevisiae* strains showed 10–60% higher antioxidation than previously reported for *S. cerevisiae* in various studies [5, 21, 27]. Moreover, in opposition to the findings of Fu et al., we do not confirm that *S. cerevisiae* displays significantly lower antioxidation than *S. boulardii*. In fact, assuming 10% confidence, WUT3 showed even a higher reduction of DPPH than SB ($p = 0.07$). It is worth mentioning that all tested yeasts had reduction properties comparable to those of the popular organic reducer HCOOH.

Antimicrobial properties and drug resistance were the last parameters in WUT3 and WUT151 strains probiotic validation. Yeast can display direct antimicrobial activity

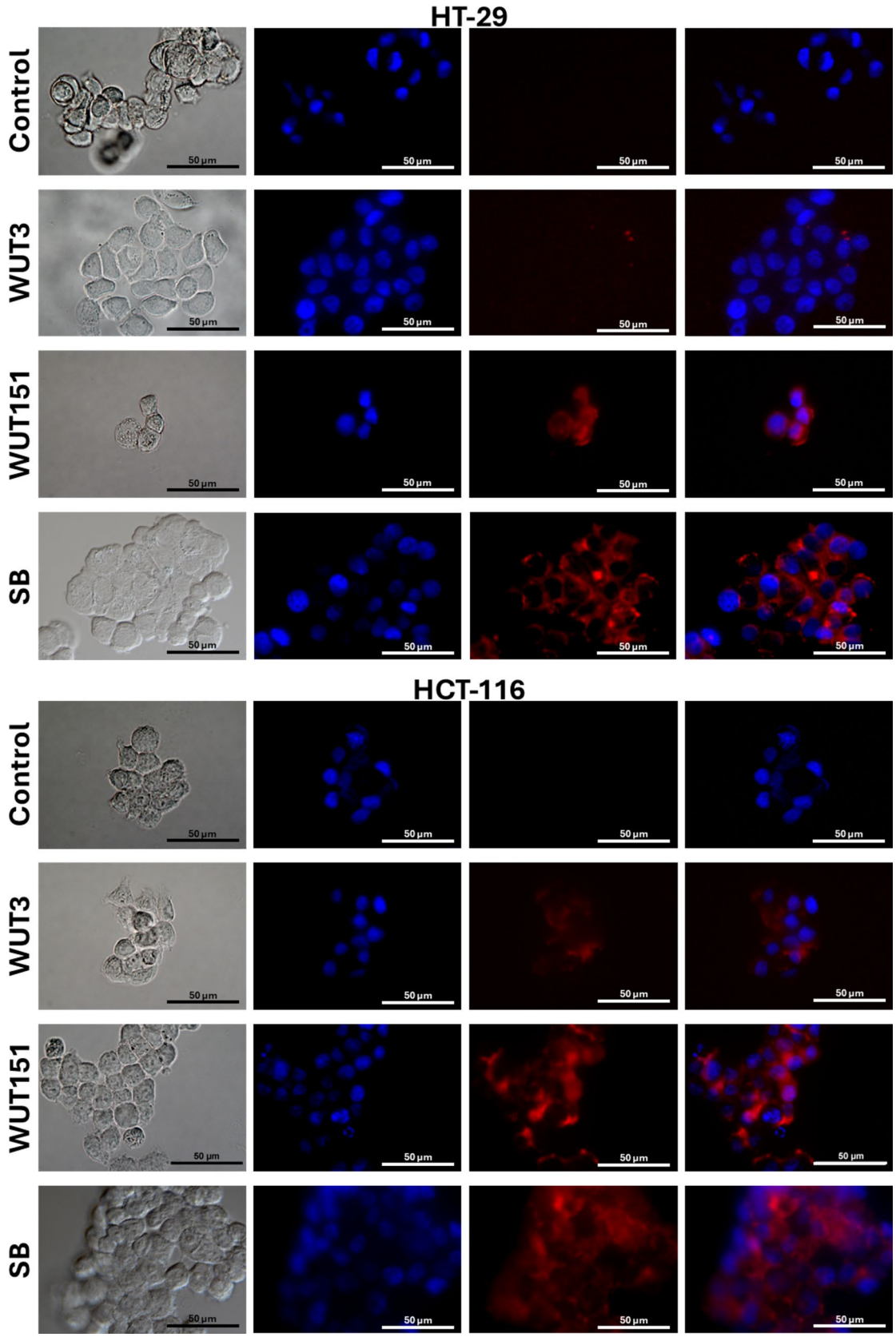
HT-29
Control
WUT3
WUT151
SB
HCT-116
Control
WUT3
WUT151
SB
50 μm

◂**Fig. 9** Interaction of Nile Red-stained yeast EVs with human HT-29 or HCT-116 cells, visualized by fluorescence microscopy. Image order (left to right): bride field, blue—channel nuclei staining (DAPI), red—channel membrane staining (EVs-Nile Red), merged. Control—PBS undergone the same staining process

due to releasing extracellular bioactive proteins such as proteases, bacteriocins, and mycocins [28, 29]. However, it is strain-specific and should be determined for each potential probiotic strain [30]. Reduction of *C. albicans* content after oral distribution of *S. cerevisiae* was previously observed in in vivo trials [31]. In this work, we did not observe significant anti-*C. albicans* activity. On the other hand, tested yeasts showed significant activity against *S. aureus* and *P. aeruginosa* and moderate antagonism to *E. coli*. Fakruddin et al. reported that *S. cerevisiae* IFST 062013 is more active against gram-negative bacteria, but a different examination method was used, and the activity difference was minor [32]. Both *S. cerevisiae* WUT3 and WUT151 strains and *S. boulardii* displayed extremely high antifungal activity, especially against *A. niger*, *F. sambucinum*, and *F. oxysporum*. Those results are consistent with the report by Hathout et al. in which *S. cerevisiae* NRRL Y-12633 strongly limited the growth of *A. niger* and *Fusarium graminearum*, among others, reaching an inhibition rate of over 85% [33].

The resistance of probiotic yeast strains to bacterial antibiotics is of great concern, particularly because of the potential to use them in antimicrobial therapy without loss of efficacy [11]. Therefore, although still overlooked by many researchers [34], there is a strong need to determine the drug resistance of potential probiotics. In our study, strains WUT3 and WUT151 of *S. cerevisiae* and a reference strain of *S. boulardii* showed resistance to commonly used antimicrobial drugs. A thorough literature analysis shows divergence in SB drug resistance, suggesting that it is strongly associated with the strain analyzed [5, 32, 35, 36]. On the other hand, probiotic yeast should be sensitive to at least one antifungal drug, especially since recent medical reports have highlighted a few cases of fungemia in patients treated with *S. cerevisiae var. boulardii* probiotics [37, 38]. Therefore, a backup tool to prevent probiotic proliferation in emergency situations seems essential. In the case of the WUT3 and WUT151 strains, they were sensitive to amphotericin B.

Our research also sought to characterize yeast EVs and investigate their interactions with human intestinal cells in vitro. The diameters of all isolated EVs were within the typical range reported for yeasts [22, 39]. EVs isolated from *S. cerevisiae* WUT3 had significantly smaller diameters than WUT151. The size of EVs is likely to be strain specific and not universal across the species, especially as EVs particles isolated from *S. cerevisiae* CL4 and CL1 were approximately 10 times more concentrated than WUT3 and had even smaller diameters (< 100 nm) [16]. The concentration of WUT151 and SB EVs were comparable to those obtained for various *S. cerevisiae* strains and other yeast species reported in the literature [16, 40, 41]. The observed variability in *S. boulardii* EVs productivity per cell may result from different culture conditions, e.g., media; in the present work, we used SAB instead of YPD [22]. The TEM images, taken using a well-established negative staining technique, showed a typical view of the EVs samples [42–47]. Besides, their positive staining with Nile Red (NR) is the factor suggesting a membrane origin of EVs. As a lipophilic dye, NR is associated with the inner elements of the phospholipid bilayer [48].

According to the EN ISO 10993–5:2009, cytotoxic potential is considered when cell viability is reduced by more than 30%. Based on this criterion, none of the tested EVs were toxic against the normal CCD-18 Co and CCD-841 CoN cell lines, indicating their safety in the human gastrointestinal tract. In the case of cancer cells, the threshold was passed for the HT-29 line but not for the HCT-116 and CaCo-2 lines. HCT-116 is reported to be a more aggressive cancer model with higher drug resistance [49]; for instance, Vemurafenib reached a tenfold lower IC_{50} for HT-29 than HCT-116 cells [50]. It was found that overexpression of transcriptional factor SOX9 may increase cancer survival. The overexpression of this gene in non-differentiated HCT-116 cells is over twice as high as in well-differentiated HT-29 [51]. This may be why EVs were toxic only against the more sensitive HT-29 cells. On the other hand, CaCo-2 is also a well-differentiated cancer cell line, but a toxic effect of yeast EVs was not observed. This cell line has enterocyte morphology and, in contrast to HT-29, does not secrete mucus [52]. Exosomes are lipophilic, while mucus is hydrophilic. Therefore, it was expected that HT-29 would be less sensitive to the potential toxic agent due to the protective mucus layer, but it was not confirmed experimentally. Reale et al. observed a similar unexpected result, where lipophilic anticancer okadaic acid was more toxic to the HT-29 cells than to the CaCo-2 [53]. This was justified by the difference in the rate of detoxification of cells, which may also be the case in our study. The lack of toxicity of WUT yeast EVs against normal human cells is the most important result. It is consistent with our previous work, where *S. boulardii* EVs also showed a lack of toxicity to normal CCD-841 CoN cells [22]. Here, we expanded the research on another normal cell line, CCD-18 Co, with analogous conclusions.

A comparison of the EVs' protein profiles showed a high similarity between all tested strains. SB EVs shared 80% less proteins with WUT3 than with WUT151, indicating that in terms of EVs protein profiles, WUT151 and SB are closer related than WUT3 and SB. The identified proteasome had over 28% ($p < 10^{-47}$) complementarity to the previously reported *S. cerevisiae* surface-exposed proteins and vacuolar luminal proteasome [54, 55]. Combined

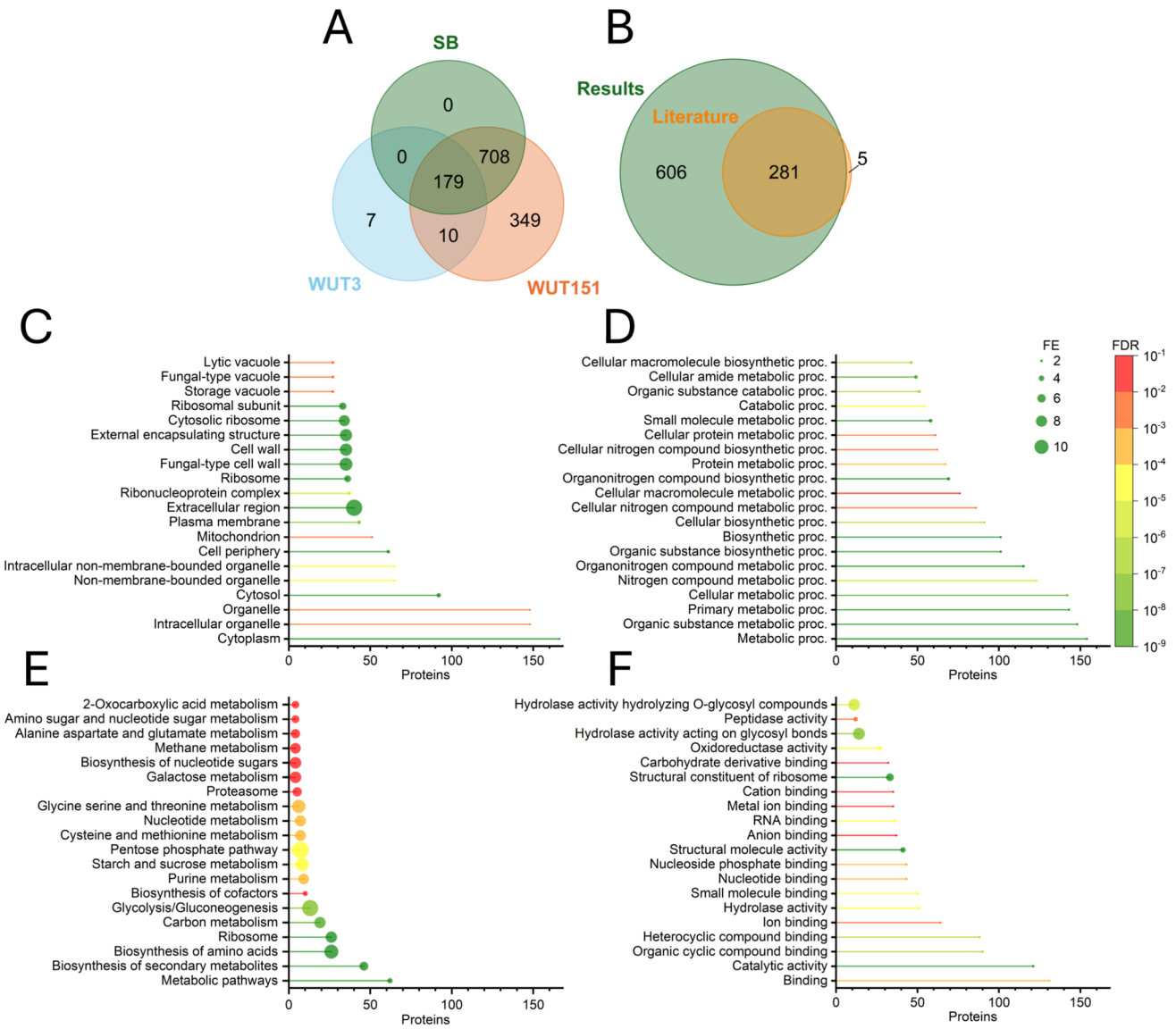

Fig. 10 Proteomic analysis of EVs isolated from WUT3, WUT151, and *S. boulardii* (SB). EVs are rich in proteins characteristic of extracellular regions. **A** Protein profile compared between tested strains. **B** Protein profile of *S. boulardii* EVs compared with the literature for the same strain [22]. **C** GO cellular component. **D** GO molecular process. **E** KEEG database enrichment. **F** GO molecular function. FE, fold enrichment; FDR, false discovery rate (lower = more significant)

with the high protein enrichment for the extracellular region, external encapsulating structure, and plasma membrane, the membrane-related origin of EVs can be confirmed. Significant overrepresentation of beta-glucan modifying enzymes and high levels of cell wall-related proteins shed some light on the cell escape mechanism of EVs. EVs may pass the cell wall barrier with partial degradation of its structure. Although it is still unclear how EV lipid structures pass through the yeast cell wall, this may be related to the β-glucan-degrading enzymes present in the various EV studies [56]. On the other hand, the cell wall components present in EVs may be associated with cell wall remodeling, which is one of the cellular responses to environmental changes [57]. The prevalence of metabolic proteins has previously been observed in yeast EVs, which is consistent with our findings [22, 57]. Each EV encapsulates some part of the cell cytosol, where glycolysis occurs. This explains why we identified enzymes fulfilling the glycolysis pathway. Another function of enzymes exported via EVs is facilitating the cell's ability to obtain nutrients. However, it is unlikely that enzymes associated with glycosylation are related to this particular function of EVs. Nevertheless, the large number of peptidases and endopeptidases we detected is remarkable in the context of nutrition [58].

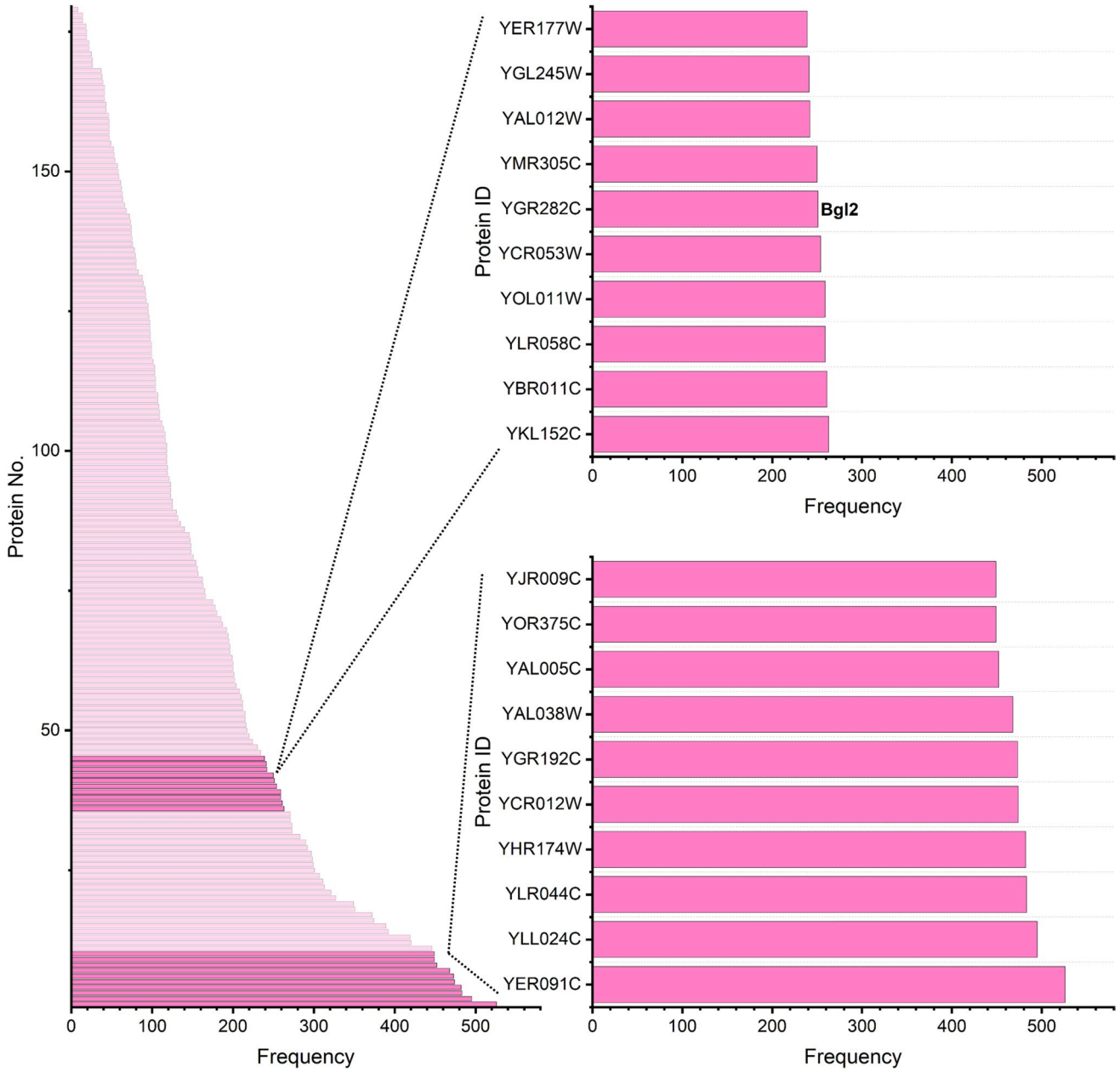

Fig. 11 The search for an *S. cerevisiae* EVs biomarker. Normalized protein detection frequency in descending order

In the search for *S. cerevisiae* EVs biomarker, the Bgl2 protein was selected as having promising properties, namely yeast-specific, directly associated with the extracellular region, and highly abundant in WUT3, WUT151, and SB EVs. To the best of our knowledge, this is the first report identifying such a protein for probiotic yeast EVs. This opens up the possibility of using more selective immunological methods to detect, isolate, and purify EVs.

Conclusion

This study provides evidence that the *S. cerevisiae* WUT3 and WUT151 strains demonstrate probiotic properties in vitro. Notably, some of their probiotic activities were superior to those of *S. cerevisiae var. boulardii* CNCM I-745, the only yeast probiotic currently approved for pharmaceutical use. Consequently, the *S. cerevisiae* WUT3 and

WUT151 appear to be promising candidates for the development of new yeast probiotics; however, their probiotic potential must be validated further using more advanced in vivo systems.

In addition, the present report indicates that the WUT3 and WUT151 strains secrete extracellular vesicles that are non-toxic to normal human colorectal model cell lines, which suggests that they will be safe for in vivo usage. Moreover, these EVs have been shown to attach to and interact with human cells in vitro. This provides a strong basis for further research into the use of these particles to carry therapeutic substances.

Supplementary Information The online version contains supplementary material available at https://doi.org/10.1007/s12602-025-10624-0.

Acknowledgements We acknowledge Julia Czopek, a student at Warsaw University of Technology, for her support in data collection. The research was carried out using equipment co-funded by the Warsaw University of Technology within the Excellence Initiative: Research University (IDUB) program. TEM studies were performed in the Laboratory of Electron Microscopy of the Nencki Institute, supported by the project financed by the Minister of Education and Science based on contract No 2022/WK/05 (Polish Euro-BioImaging Node "Advanced Light Microscopy Node Poland").

Author Contribution A.G., J.M., M.R.: Conceptualization. A.G., J.M., M.R., M.M.K., E.S., M.B., M.E.Ś.: Methodology. A.G., E.S., M.B., M.E.Ś., J.M.: Investigation, Data acquisition. A.G., M.K.B.: Data analysis, Data visualization. A.G., M.K.B.: Statistical analysis. J.M.: Funding acquisition, Supervision. A.G.: Writing - main text. A.G., J.M., M.M.K.: Writing – revision and editing. All authors: review.

Funding This work is part of the "Extracellular vesicles of probiotic yeast as carriers of biologically active molecules transferred to human intestinal cells" project funded by the National Science Centre, Poland (NCN). The project is being implemented under No. 2023/49/B/NZ9/03663.

Data Availability No datasets were generated or analysed during the current study.

Declarations

Competing interests The authors declare no competing interests.

References

1. Morelli L, Capurso L (2012) FAO/WHO guidelines on probiotics: 10 years later. J Clin Gastroenterol 46:S1–S2. https://doi.org/10.1097/MCG.0b013e318269fdd5
2. Mazziotta C, Tognon M, Martini F, Torreggiani E, Rotondo JC (2023) Probiotics mechanism of action on immune cells and beneficial effects on human health. Cells 12:184. https://doi.org/10.3390/cells12010184
3. Wieërs G, Belkhir L, Enaud R, Leclercq S, Philippart de Foy JM, Dequenne I, de Timary P, Cani PD. How probiotics affect the microbiota (2020) Front Cell Infect Microbiol 9:454. https://doi.org/10.3389/fcimb.2019.00454.
4. Stavropoulou E, Bezirtzoglou E (2020) Probiotics in medicine: a long debate. Front Immunol 11:2192. https://doi.org/10.3389/fimmu.2020.02192
5. Hossain MN, Afrin S, Humayun S, Ahmed MM, Saha BK (2020) Identification and growth characterization of a novel strain of Saccharomyces boulardii isolated from soya paste. Front Nutr 7:27. https://doi.org/10.3389/fnut.2020.00027
6. Staniszewski A, Kordowska-Wiater M (2021) Probiotic and potentially probiotic yeasts—characteristics and food application. Foods 10:1306. https://doi.org/10.3390/foods10061306
7. Kil BJ, Pyung YJ, Park H, Kang J-W, Yun C-H, Huh CS (2023) Probiotic potential of Saccharomyces cerevisiae GILA with alleviating intestinal inflammation in a dextran sulfate sodium induced colitis mouse model. Sci Rep 13:6687. https://doi.org/10.1038/s41598-023-33958-7
8. Probiotics Database. Available from: https://www.optibacprobiotics.com/professionals/probiotics-database. Accessed 27 May 2025
9. McFarland LV (1996) Saccharomyces boulardii is not Saccharomyces cerevisiae. Clin Infect Dis 22:200–201. https://doi.org/10.1093/clinids/22.1.200
10. Fietto JLR, Araújo RS, Valadão FN, Fietto LG, Brandão RL, Neves MJ, Gomes FCO, Nicoli JR, Castro IM (2004) Molecular and physiological comparisons between *Saccharomyces Cerevisiae* and *Saccharomyces Boulardii*. Can J Microbiol 50:615–621. https://doi.org/10.1139/w04-050
11. Ansari F, Alian Samakkhah S, Bahadori A, Jafari SM, Ziaee M, Khodayari MT, Pourjafar H (2023) Health-promoting properties of *Saccharomyces cerevisiae var. boulardii* as a probiotic; characteristics, isolation, and applications in dairy products. Crit Rev Food Sci and Nutr 63:457–485. https://doi.org/10.1080/10408398.2021.1949577
12. Sen S, Mansell TJ (2020) Yeasts as probiotics: mechanisms, outcomes, and future potential. Fungal Genet Biol 137:103333. https://doi.org/10.1016/j.fgb.2020.103333
13. ClinicalTrials.gov. Available from: https://clinicaltrials.gov/. Accessed 7 June 2024
14. Mencher A, Morales P, Valero E, Tronchoni J, Patil KR, Gonzalez R (2020) Proteomic characterization of extracellular vesicles produced by several wine yeast species. Microb Biotechnol 13:1581–1596. https://doi.org/10.1111/1751-7915.13614
15. Welsh JA, Goberdhan DCI, O'Driscoll L, Buzas EI, Blenkiron C, Bussolati B, Cai H, Di Vizio D, Driedonks TAP, Erdbrügger U et al (2024) Minimal information for studies of extracellular vesicles (MISEV2023): from basic to advanced approaches. J of Extracellular Vesicle 13:e12404. https://doi.org/10.1002/jev2.12404
16. Nenciarini S, Amoriello R, Bacci G, Cerasuolo B, Di Paola M, Nardini P, Papini A, Ballerini C, Cavalieri D (2024) Yeast strains isolated from fermented beverage produce extracellular vesicles with anti-inflammatory effects. Sci Rep 14:730. https://doi.org/10.1038/s41598-024-51370-7

17. Chreptowicz K, Wielechowska M, Główczyk-Zubek J, Rybak E, Mierzejewska J (2016) Production of Natural 2-phenylethanol: from biotransformation to purified product. Food Bioprod Process 100:275–281. https://doi.org/10.1016/j.fbp.2016.07.011
18. Chen L, Deng R, Yokoyama W, Zhong F (2022) Investigation of the effect of nanocellulose on delaying the in vitro digestion of protein, lipid, and starch. Food Hydrocolloids for Health 2:100098. https://doi.org/10.1016/j.fhfh.2022.100098
19. Marques MRC, Loebenberg R, Almukainzi M (2011) Simulated biological fluids with possible application in dissolution testing. Dissolution Technol 18:15–28. https://doi.org/10.14227/DT180311P15
20. Garcia-Gonzalez N, Prete R, Battista N, Corsetti A (2018) Adhesion properties of food-associated Lactobacillus plantarum strains on human intestinal epithelial cells and modulation of IL-8 release. Front Microbiol 9:2392. https://doi.org/10.3389/fmicb.2018.02392
21. Fu J, Liu J, Wen X, Zhang G, Cai J, Qiao Z, An Z, Zheng J, Li L (2023) Unique probiotic properties and bioactive metabolites of Saccharomyces boulardii. Probiotics & Antimicro Prot 15:967–982. https://doi.org/10.1007/s12602-022-09953-1
22. Mierzejewska J, Kowalska P, Marlicka K, Dworakowska S, Sitkiewicz E, Trzaskowski M, Głuchowska A, Mosieniak G, Milner-Krawczyk M (2023) Exploring extracellular vesicles of probiotic yeast as carriers of biologically active molecules transferred to human intestinal cells. IJMS 24:11340. https://doi.org/10.3390/ijms241411340
23. Hughes CS, Foehr S, Garfield DA, Furlong EE, Steinmetz LM, Krijgsveld J (2014) Ultrasensitive proteome analysis using paramagnetic bead technology. Mol Syst Biol 10:757. https://doi.org/10.15252/msb.20145625
24. Krzyżek P, Marinacci B, Vitale I, Grande R (2023) Extracellular vesicles of probiotics: shedding light on the biological activity and future applications. Pharmaceutics 15:522. https://doi.org/10.3390/pharmaceutics15020522
25. Suvarna S, Dsouza J, Ragavan ML, Das N (2018) Potential probiotic characterization and effect of encapsulation of probiotic yeast strains on survival in simulated gastrointestinal tract condition. Food Sci Biotechnol 27:745–753. https://doi.org/10.1007/s10068-018-0310-8
26. Meng Y, Zhang L, Li P, Yu J, Mu G, Li X, Tuo Y (2022) Saccharomyces cerevisiae I4 showed alleviating effects on dextran sulfate sodium-induced colitis of Balb/c mice. Foods 11:1436. https://doi.org/10.3390/foods11101436
27. Menezes AGT, Ramos CL, Cenzi G, Melo DS, Dias DR, Schwan RF (2020) Probiotic potential, antioxidant activity, and phytase production of indigenous yeasts isolated from indigenous fermented foods. Probiotics & Antimicro Prot 12:280–288. https://doi.org/10.1007/s12602-019-9518-z
28. Branco P, Maurício EM, Costa A, Ventura D, Roma-Rodrigues C, Duarte MP, Fernandes AR, Prista C (2023) Exploring the multifaceted potential of a peptide fraction derived from Saccharomyces cerevisiae metabolism: antimicrobial, antioxidant, antidiabetic, and anti-inflammatory properties. Antibiotics 12:1332. https://doi.org/10.3390/antibiotics12081332
29. Cotter PD, Hill C, Ross RP (2005) Bacteriocins: developing innate immunity for food. Nat Rev Microbiol 3:777–788. https://doi.org/10.1038/nrmicro1273
30. Gaziano R, Sabbatini S, Roselletti E, Perito S, Monari C (2020) Saccharomyces cerevisiae-based probiotics as novel antimicrobial agents to prevent and treat vaginal infections. Front Microbiol 11:718. https://doi.org/10.3389/fmicb.2020.00718
31. Pericolini E, Gabrielli E, Ballet N, Sabbatini S, Roselletti E, Cayzeele Decherf A, Pélerin F, Luciano E, Perito S, Jüsten P et al (2017) Therapeutic activity of a *Saccharomyces Cerevisiae* -based probiotic and inactivated whole yeast on vaginal candidiasis. Virulence 8:74–90. https://doi.org/10.1080/21505594.2016.1213937
32. Fakruddin Md, Hossain MdN, Ahmed MM (2017) Antimicrobial and antioxidant activities of Saccharomyces cerevisiae IFST062013, a potential probiotic. BMC Complement Altern Med 17:64. https://doi.org/10.1186/s12906-017-1591-9
33. Hathout A, Abdel-Nasser A (2022) The efficiency of Saccharomyces cerevisiae as an antifungal and antimycotoxigenic agent. Biointerface Res Appl Chem 13:355. https://doi.org/10.33263/BRIAC134.354
34. Kunyeit L, Rao RP, Anu-Appaiah KA (2023) Yeasts originating from fermented foods, their potential as probiotics and therapeutic implication for human health and disease. Crit Rev Food Sci Nutr 64:6660–6671. https://doi.org/10.1080/10408398.2023.2172546
35. Sharma J, Goyal A (2015) A study on the drug resistance of probiotic strains isolated from commercial probotic products available in the local market of Agra. Eur J Exp Biol 5:33–36
36. Selvin J, Maity D, Sajayan A, Kiran GS (2020) Revealing antibiotic resistance in therapeutic and dietary probiotic supplements. Journal of Global Antimicrobial Resistance 22:202–205. https://doi.org/10.1016/j.jgar.2020.02.007
37. Rannikko J, Holmberg V, Karppelin M, Arvola P, Huttunen R, Mattila E, Kerttula N, Puhto T, Tamm Ü, Koivula I et al (2021) Fungemia and other fungal infections associated with use of *Saccharomyces Boulardii* probiotic supplements. Emerg Infect Dis 27:2043–2051. https://doi.org/10.3201/eid2708.210018
38. Piotrowski M, Wultańska D, Pituch H (2022) Effect of prebiotics on *Bacteroides* sp. adhesion and biofilm formation and synbiotic effect on *Clostridioides difficile*. Future Microbiol 17:363–375. https://doi.org/10.2217/fmb-2021-0206
39. Rogers NMK, Hicks E, Kan C, Martin E, Gao L, Limso C, Hendren CO, Kuehn M, Wiesner MR (2023) Characterizing the transport and surface affinity of extracellular vesicles isolated from yeast and bacteria in well-characterized porous media. Environ Sci Technol 57:13182–13192. https://doi.org/10.1021/acs.est.3c03700
40. Mejias-Ortiz M, Mencher A, Morales P, Tronchoni J, Gonzalez R (2023) *Saccharomyces cerevisiae* responds similarly to co-culture or to a fraction enriched in *Metschnikowia pulcherrima* extracellular vesicles. Microb Biotechnol 16:1027–1040. https://doi.org/10.1111/1751-7915.14240
41. Kulig K, Kowalik K, Surowiec M, Karnas E, Barczyk-Woznicka O, Zuba-Surma E, Pyza E, Kozik A, Rapala-Kozik M, Karkowska-Kuleta J (2024) Isolation and characteristics of extracellular vesicles produced by probiotics: yeast Saccharomyces boulardii CNCM I-745 and bacterium Streptococcus salivarius K12. Probiotics & Antimicro Prot 16:936–948. https://doi.org/10.1007/s12602-023-10085-3
42. Wei B, Xiang Y, Qin X, Yang Y, Lu H, Li H, Fang M, Li X, Yang F (2024) EVs-on-a-bubble: self-aggregated click bubbles streamline isolation and amplified profiling of circulating extracellular vesicles. Adv Funct Materials 34:2310823. https://doi.org/10.1002/adfm.202310823
43. Tao X, Xu Z, Tian H, He J, Wang G, Tao X (2024) Differential proteins from EVs identification based on tandem mass tags analysis and effect of treg-derived EVs on T-lymphocytes in COPD patients. Respir Res 25:349. https://doi.org/10.1186/s12931-024-02980-2
44. Nikishin I, Dulimov R, Skryabin G, Galetsky S, Tchevkina E, Bagrov D (2021) ScanEV – a neural network-based tool for the automated detection of extracellular vesicles in TEM images. Micron 145:103044. https://doi.org/10.1016/j.micron.2021.103044
45. Huang M, Zheng M, Song Q, Ma X, Zhang Q, Chen H, Jiang G, Zhou S, Chen H, Wang G et al (2024) Comparative proteomics inspired self-stimulated release hydrogel reinforces the

therapeutic effects of MSC-EVs on Alzheimer's disease. Adv Mater 36:2311420. https://doi.org/10.1002/adma.202311420
46. Bagrov DV, Senkovenko AM, Nikishin II, Skryabin GO, Kopnin PB, Tchevkina EM (2021) Application of AFM, TEM, and NTA for characterization of exosomes produced by placenta-derived mesenchymal cells. J Phys Conf Ser 1942. https://doi.org/10.1088/1742-6596/1942/1/012013
47. Badrhan S, Karanwal S, Pal A, Chera JS, Chauhan V, Patel A, Bhakat M, Datta TK, Kumar R (2024) Differential protein repertoires related to sperm function identified in extracellular vesicles (EVs) in seminal plasma of distinct fertility buffalo (Bubalus bubalis) Bulls. Front Cell Dev Biol 12:1400323. https://doi.org/10.3389/fcell.2024.1400323
48. Domínguez-Arca V, Costa RR, Carvalho AM, Taboada P, Reis RL, Prieto G, Pashkuleva I (2021) Liposomes embedded in layer by layer constructs as simplistic extracellular vesicles transfer model. Mater Sci Eng, C 121:111813. https://doi.org/10.1016/j.msec.2020.111813
49. Pakdemirli A, Karaca C, Sever T, Daşkin E, Leblebici A (2020) Carvacrol alters soluble factors in HCT-116 and HT-29 cell lines. Turk J Med Sci. https://doi.org/10.3906/sag-1907-173
50. Cordeiro HG, De Sousa Faria AV, Ferreira-Halder CV (2020) Vemurafenib downmodulates aggressiveness mediators of colorectal cancer (CRC): low molecular weight protein tyrosine phosphatase (LMWPTP), protein tyrosine phosphatase 1B (PTP1B) and transforming growth factor β (TGF β). Biol Chem 401:1063–1069. https://doi.org/10.1515/hsz-2020-0124
51. Lizárraga-Verdugo E, Ruiz-García E, López-Camarillo C, Bermúdez M, Avendaño-Félix M, Ramos-Payán R, Romero-Quintana G, Ayala-Ham A, Villegas-Mercado C, Pérez-Plasencia C et al (2020) Cell survival is regulated via SOX9/BCL2L1 axis in HCT-116 colorectal cancer cell line. Journal of Oncology 2020:1–10. https://doi.org/10.1155/2020/5701527
52. Gagnon M, Zihler Berner A, Chervet N, Chassard C, Lacroix C (2013) Comparison of the Caco-2, HT-29 and the mucus-secreting HT29-MTX intestinal cell models to investigate salmonella adhesion and invasion. J Microbiol Methods 94:274–279. https://doi.org/10.1016/j.mimet.2013.06.027
53. Reale O, Huguet A, Fessard V (2021) Co-culture model of Caco-2/HT29-MTX cells: a promising tool for investigation of phycotoxins toxicity on the intestinal barrier. Chemosphere 273:128497. https://doi.org/10.1016/j.chemosphere.2020.128497
54. Marino SM, Li Y, Fomenko DE, Agisheva N, Cerny RL, Gladyshev VN (2010) Characterization of surface-exposed reactive cysteine residues in *Saccharomyces cerevisiae*. Biochemistry 49:7709–7721. https://doi.org/10.1021/bi100677a
55. Sarry J, Chen S, Collum RP, Liang S, Peng M, Lang A, Naumann B, Dzierszinski F, Yuan C, Hippler M et al (2007) Analysis of the vacuolar luminal proteome of *Saccharomyces cerevisiae*. FEBS J 274:4287–4305. https://doi.org/10.1111/j.1742-4658.2007.05959.x
56. Oliveira DL, Nakayasu ES, Joffe LS, Guimarães AJ, Sobreira TJP, Nosanchuk JD, Cordero RJB, Frases S, Casadevall A, Almeida IC et al (2010) Biogenesis of extracellular vesicles in yeast: many questions with few answers. Communicative & Integrative Biology 3:533–535. https://doi.org/10.4161/cib.3.6.12756
57. Karkowska-Kuleta J, Kulig K, Karnas E, Zuba-Surma E, Woznicka O, Pyza E, Kuleta P, Osyczka A, Rapala-Kozik M, Kozik A (2020) Characteristics of extracellular vesicles released by the pathogenic yeast-like fungi Candida glabrata. Candida Parapsilosis and Candida tropicalis Cells 9:1722. https://doi.org/10.3390/cells9071722
58. Bertels LK, Fernández Murillo L, Heinisch JJ (2021) The pentose phosphate pathway in yeasts–more than a poor cousin of glycolysis. Biomolecules 11:725. https://doi.org/10.3390/biom11050725